TP 7740E

TESTING OF A MOLICEL® LITHIUM/MOLYBDENUM DISULPHIDE BC SIZE BATTERY

Prepared For:

Transportation Development Centre
Transport Canada

By:

Moli Energy Limited

July 19, 1986

Library and Information Centre /
Centre de Documentation (CDLI)
RECEIVED - REÇU LE
SEP 10 19
Transport Canada / Transports Canada

TP 7740E

TESTING OF A MOLICEL® LITHIUM/MOLYBDENUM DISULPHIDE BC SIZE BATTERY

BY:

J. BRYAN TAYLOR

MOLI ENERGY LIMITED
3958 Myrtle Street
Burnaby, B.C. V5C 4G2
Canada

July 19, 1986

The contents of this report reflect the views of Moli Energy Limited and not necessarily the official view or opinions of the Transportation Development Centre of Transport Canada.

MOLI and MOLICEL are registered trademarks of Moli Energy Limited.

Un sommaire en français de ce rapport est inclus avant la Table des matières.

PROJECT TEAM

The following Moli Energy Personnel have contributed to the work reported herein. The author gratefully acknowledges the work done by these persons and by their support staff listed below.

D. Wainwright (Project Leader)
W. Chow
R. Shimizu

D. Fouchard (Safety Testing)
A. Marr
H. Woo
P. Howell

L. Ruggier (Thermal Modelling)

M. Reid (Electronics and Data Systems)
K. Wong
R. Johnson

D. Roberts (Model Plant/Cell Fabrication)
B. Wong
C. Weiz

C. Laborie (Design and Mechanical Engineering)
J. Allen
A. Shkuratoff
D. Ironmonger
D. Chang
E. Wildenboer

REPORT DOCUMENTATION FORM

1. Transport Canada Report No.	2. TDC Project No.	3. Recipient's Catalogue No.
TP 7740E	6332	

4. Title and Subtitle	5. Report Date
TESTING OF A MOLICEL® LITHIUM/MOLYBDENUM DISULPHIDE BC SIZE BATTERY	MAY 1986
	6. Performing Organization Report No
7. Author(s) DR. J.B. TAYLOR	8. Transport Canada File No D 1465-416-5
9. Performing Organization Name and Address MOLI ENERGY LIMITED 3958 Myrtle Street Burnaby, B.C. V5C 4G2	10. DSS File No 08 SB T8200-4-4653
	11. DSS or Transport Canada Contract No 0 SB 84-00654
12. Sponsoring Agency Name and Address TRANSPORTATION DEVELOPMENT CENTRE Guy Favreau Complex 200 Dorchester Blvd. West, Suite 601 West Tower Montreal, Quebec H2Z 1X4	13. Type of Report and Period Covered FINAL
	14. Sponsoring Agency Code
15. Supplementary Notes	16. TDC Project Officer J.H. Morgan

17. Abstract

Large rechargeable lithium/molybdenum disulphide cells have been designed, built and tested to determine their suitability for electric vehicle batteries. The tests were made on scaled versions of the standard MOLICEL technology with appropriate modifications to meet the specific peak power demands of an electric vehicle duty cycle. The cells had a nominal capacity of 50 Ah and were found to have a specific energy of 60 Wh/kg at a specific power of 20 W/kg. The specific peak power was found to be 200 W/kg. Comparisons have been made with performance data for other batteries of possible applicability to electric traction. The MOLICELs were found to have performance advantages and were apparently suitable for electric vehicle use. This has been confirmed by subjecting cells to testing based on simulated duty cycles derived from analysis of the needs of a conceptual small two-passenger vehicle.

The large power capability of these cells can create safety concerns particularly under conditions of severe electrical abuse where excessive thermal power dissipation causes unacceptable heat build-up. Thermal studies have indicated that this heat can be removed. Thus with appropriate design modifications, the 50 Ah MOLICEL can form the basis of a practical electric vehicle battery.

18. Key Words	19. Distribution Statement
RECHARGEABLE LITHIUM BATTERIES, ELECTRIC VEHICLE BATTERIES, BATTERY TESTING, BATTERY PERFORMANCE, BATTERY SAFETY	A LIMITED NUMBER OF COPIES AVAILABLE FROM TDC ON REQUEST.

20. Security Classification (of this report)	21. Security Classification (of this page)	22. No. of Pages	23. Price
NONE	NONE		NIL

FORMULE DE DOCUMENTATION POUR RAPPORT

1. N° du rapport Transports Canada	2. N° de l'étude — CDT	3. N° de catalogue du destinataire
TP 7740E	6332	

4. Titre et sous-titre	5. Date du rapport
Essais de la pile MOLICEL® de format BC au lithium-disulfure de molybdène.	MAI 1986
	6. N° du rapport de l'organisme exécutant

7. Auteur(s)	8. N° de dossier Transports Canada
DR. J.B. TAYLOR	D 1465-416-5

9. Nom et adresse de l'organisme exécutant	10. N° de dossier — ASC
MOLI ENFRGY LIMITED 3958 Myrtle Street Burnaby, B.C. V5C 4G2	08 SB T8200-4-4653
	11. N° de contrat — ASC ou Transports Canada
	0 SB 84-00654

12. Nom et adresse de l'organisme parrain	13. Genre de rapport et période visée
CENTRE DE DEVELOPPEMENT DES TRANSPORTS COMPLEXE GUY FAVREAU 200 ouest, boul. Dorchester, Suite 601, tour ouest Montreal, Quebec H2Z 1X4	14. Code de l'organisme parrain

15. Remarques additionnelles	16. Agent de projet — CDT
	J.H. Morgan

17. Résumé

Une batterie rechargeable lithium-disulfure de molybdène a été conçue, réalisée et essayée dans l'optique de la traction électrique routière. Ces essais ont été faits sur des spécimens de la batterie standard MOLICEL modifiée de manière à fournir les valeurs d'énergie massique exigées en exploitation routière selon un cycle normalisé. Produisant 50 Ah, cette batterie possède une énergie massique de 60 Wh/Kg et une puissance massique de 20 W/Kg, tout en étant capable de pointes de 200 W/Kg. Son rendement, comparé à celui d'autres batteries de traction, a été supérieur et la rend apte à la traction électrique routière. Pour le confirmer, des essais ont été élaborés par voie de simulation de cycles d'exploitation normalisés basés sur les caractéristiques d'une petite voiture de tourisme deux places.

Toutefois, la grande puissance massique de la batterie peut créer en régime d'utilisation abusif certains problèmes thermiques dus à une forte accumulation de chaleur. Des études de modélisation thermique montrent qu'il est cependant possible de dissiper cette chaleur; ainsi, une batterie MOLICEL 50 Ah équipée d'un dispositif de refroidissement adéquat peut constituer une source d'énergie pratique pour la traction électrique routière.

18. Mots-clés	19. Diffusion
Batterie rechargeable, lithium-disulfure de molybdène, pile à combustible, traction électrique.	Un nombre limité de copies est disponible sur demande au centre de développement des transports.

20. Classification de sécurité (de ce rapport)	21. Classification de sécurité (de cette page)	22. Nombre de pages	23. Prix
NUL	NUL		NUL

ACKNOWLEDGEMENT

Three meetings were held with the project steering committee. Much stimulating discussion accompanied these meetings. The advice and valued contributions of all the following participants are gratefully acknowledged.

J.H. Morgan (Chairman)	- Transportation Development Centre, Transport Canada, Montreal
W. Adams	- Department of Defense, Ottawa
M. Hammerli	- National Research Council, Ottawa
J. Edwards	- National Research Council, Vancouver
W. McGarry	- Canadian Electrical Association/ Energy Mines and Resources, Ottawa
L.A. Snider	- B.C. Hydro, Vancouver
P. Boetzkes	- Consultant, North Vancouver
J. Weibe	- Department of Regional Industrial Expansion, Vancouver

SUMMARY

A large 50 Ah BC size cell based on the MOLICEL rechargeable lithium battery technology has been redesigned to achieve optimum specific power consistent with a maximum possible specific energy. A detailed performance test matrix has been developed to evaluate cell performance for electric vehicle applications. Special equipment has been designed and built to undertake the required tests. The test results show that the BC cell has an energy capacity of 60 Wh/kg at a power of 20 W/kg. It has a peak power capability of 200 W/kg. These data have been compared with the best available data for Pb/acid, Ni/Zn, Ni/Fe, and Li/FeS systems. The results show that BC MOLICELs have performance superior to all but the Li/FeS cells. On the basis of an analysis of electric vehicle power requirements for standard driving cycles, it has been concluded that a battery comprised of BC MOLICELs would give acceptable range (154 km) on an SAE J227(a) schedule D driving cycle for a specific test vehicle. Consideration of the requirement to utilize fully the MOLICEL performance characteristics leads to the conclusion that the best performance would be obtained in a small (<1000 kg) two-passenger vehicle having a design top speed of 48 km/h with possible excursions to 72 km/h. A duty cycle tester was used to simulate the SAE J227(a) schedules C & D in order to determine the expected MOLICEL performance under practical conditions. The results showed that the small two passenger vehicle with a battery weighing 225 kg and comprised of 180 BC size MOLICELs would travel 42 km on one charge. It would execute all the requirements of schedule C and would suffer no range penalties with occasional power excursions associated with hill climbing or higher speeds.

The issue of safety remains unresolved for BC cells of the present design. As a result of their energy content and high power capabilities, short circuit currents of 250 amperes are possible. Large amounts of heat are generated internally on short circuit and if not dissipated, the cell active materials start to react directly causing a venting with very strong burning. Thermal studies based on experimental measurements have shown that there are ways in which this heat can be removed. Model studies indicate that quite simple cooling systems will be able to handle the short circuit heat flux and hold the cells below the temperature at which severe venting occurs. These concepts remain untested, but present indications are that incorporation of suitable thermal management will be possible in a modified BC cell and such a cell can form the basis of a practical electric vehicle battery.

SOMMAIRE

La batterie rechargeable lithium-disulfure de molybdène MOLICEL de taille "BC" produisant 50 Ah a été réétudiée en vue de lui donner une puissance massique optimale, en meme temps qu'une énergie massique maximum. Afin d'en connaitre les performances en traction routière électrique, une matrice d'essais a été étudiée tandis qu'un équipement spécialisé a été conçu et réalisé exprès. Les essais ont montré que la batterie possède une énergie massique de 60 Wh/kg et une puissance massique de 20 W/kg tout en étant capable de pointes de 200 W/kg. Le rendement, comparé aux meilleurs résultats connus des batteries plomb-acide, Ni-Zn, Ni-Fe et Li-FeS, a été supérieur dans tous les cas, sauf le dernier. Une analyse des besoins énergétiques pour la traction électrique routière en cycles d'exploitation standard a permis de constater qu'une batterie MOLICEL donnerait au véhicule d'essai exploité en cycle normalisé SAE J227(a) D une autonomie de 154 km, ce qui est jugé acceptable. Une étude attentive a fait ressortir que le véhicule le mieux adapté aux caractéristiques de la batterie MOLICEL serait une voiture de tourisme deux places, pesant moins d'un millier de kg, et affichant une vitesse maximum théorique de 48 km/h avec des pointes de 72 km/h. Un montage a été réalisé pour simuler les performances de cette batterie exploitée dans des conditions de service correspondant aux cycles normalisés J227(a) C et D. Les résultats ont montré que le véhicule deux places équipé d'une batterie de 225 kg formée de 180 cellules MOLICEL de taille BC aurait une autonomie de 42 km. Elle pourrait satisfaire au cycle C sans restriction aucune, tout en étant capable de fournir les pointes nécessaires au dépassement et au franchissement de rampes.

En revanche, l'aspect sécurité des batteries de taille BC n'a pas encore été entièrement réglé. En effet, vu les valeurs élevées d'énergie et de puissance massiques, des courants de court circuit de 250 A sont possibles, avec un dégagement thermique interne important, lequel, s'il n'est pas dissipé, provoquerait une forte réaction chimique suivie d'un dégagement gazeux brulant. Des études théoriques complétées d'expérimentations montrent qu'il existe des méthodes pour dissiper cette chaleur. Les modèles thermiques élaborés laissent croire qu'il suffirait d'un circuit de refroidissement relativement simple pour faire disparaitre le flux thermique provoqué par un court circuit et ainsi garder la batterie à une température au-dessous de laquelle un dégagement gazeux se produit. Bien qu'aucune de ces méthodes n'ait encore été vérifiée, il est possible d'équiper une batterie modifiée d'un dispositif de refroidissement adéquat, réalisant ainsi une source d'énergie pratique pour la traction routière électrique.

TABLE OF CONTENTS

	Page
DISCLAIMER	ii
LANGUAGE	ii
PROJECT TEAM	iii
REPORT DOCUMENTATION FORM	iv
FORMULE DE DOCUMENTATION POUR RAPPORT	v
ACKNOWLEDGEMENT	vi
SUMMARY	vii
SOMMAIRE	viii
TABLE OF CONTENTS	ix, x
1. INTRODUCTION	1
1.1 Previous Work	1
1.2 Objectives of New Work	1
2. HARDWARE DEVELOPMENT	3
3. PERFORMANCE TESTS AND EQUIPMENT	9
3.1 Cycling System	9
3.2 Peak Power Tester	11
3.3 Constant Power Discharge System	12
3.4 Duty Cycler	14
4. PERFORMANCE TEST RESULTS	15
4.1.1 Capacity vs. Cycle Number	15
4.1.2 Capacity vs. Temperature	17
4.1.3 Capacity vs. Current	17
4.2.1 Peak Power vs. Depth-of-Discharge	19
4.2.2 Peak Power vs. Temperature	20
4.3 Power vs. Energy	21
4.4 Duty Cycle	25
5. SAFETY TESTING	28
5.1 Vibration	30
5.2 Shock	30
5.3 Overheating	31
5.4 Overcharge	32
5.5 Forced Discharge	34
5.6 Short Circuit	35
5.7 Crush	37
5.8 Incineration	37

TABLE OF CONTENTS (con't)

		Page
6.	**THERMAL ANALYSIS**	37
	6.1 Thermal Power	37
	6.2 Thermal Model	38
	6.3 Heat Flow Modification	39
	6.4 Alternative Thermal Management	40
7.	**COMPARATIVE BATTERY PERFORMANCE IN ELECTRIC VEHICLE APPLICATIONS**	42
	7.1 E.V. Performance Estimation	42
	7.2 Comparative Data	44

1. INTRODUCTION

1.1 Previous Work

Work for the Canadian Electrical Association and for the Transportation Development Centre of Transport Canada was completed in 1985. Its principal objective was to demonstrate the feasibility of scale up of the Moli Energy technology from a C cell size (2.3 Ah) to a much larger BC (beer can) size (40 Ah) cell. The basic technology consists of a spirally wound sandwich of lithium foil, porous separator and cathode foil. The cathode of molybdenum disulphide powder is coated onto aluminum foil which serves as a current collector. Its exact composition and form is covered by MOLI patents as is the method of making the electrochemical cell.

The scaling of this technology was achieved and satisfactory performance of single cells and of a two cell and a six cell battery pack was demonstrated. The principle performance parameters of concern were the energy density and power density. It was shown that a gravimetric energy density of 94 Wh/kg could be achieved with a power density of 128W/kg. The latter figure was stated to be capable of being improved with hardware redesign since the main limiting factor derives from resistive losses and not from intrinsic electrochemical constraints.

Safety testing was performed to investigate the effects of mechanical and electrical abuse. It became clear that the large cells could not dissipate heat quickly enough to prevent a severe venting on short circuit. Similarly after about 300% overdischarge or 50% overcharge, internal heat generation exceeded the dissipatic rate. It was concluded that thermal management could provide a solution to this problem and greatly increase the abuse tolerance of BC cells. Although it was not specifically stated, one could conceive a situation where a thermally managed system would provide a way of avoiding the performance penalties occurring below -10^{o}C.

At the conclusion of the project, the following areas of uncertainty were identified.

- Power capability of MOLICELs.
- Possibility of thermal management.
- Feasibility of using MOLICELs in electric vehicles.

1.2 Objectives of New Work

Having established the ability to scale MOLICEL technology, the developmental needs for larger cells are greatly reduced. All improvements and testing related to the basic technology development can be made using small cells. At Moli Energy, the

main developmental cell is currently the AA size. This particular size is now in the final stages of engineering development prior to commercialization in 1987. Very few contenders for the electric vehicle battery market offer such a desirably simple development option. Not only can changes be made cheaply but the unit costs associated with small cells mean that quantity fabrication and testing are possible, to give statistical significance to the data and to speed up the process of development. Furthermore, the availability of a fully engineered cell as a test vehicle means that small performance improvements are not lost in a wide deviation spread so commonly encountered in research or developmental cell data.

As a result of recognition of the foregoing and a realization of the fast pace of development of the MOLICEL technology as it approaches commercialization, it was decided to concentrate large cell development and testing as follows:

1.2.1 Optimization of power capability.
1.2.2 Thermal testing prior to cell redesign.
1.2.3 Electric vehicle applications analysis and comparative EV battery data base.

The stated objective of the present project is as follows:

> "To advance the range and performance of electric vehicles by undertaking a comprehensive series of output and reliability tests on newly developed $LiMoS_2$ batteries".

To undertake this work some cell redesign had to be done. In fact three design iterations were completed and the cells from each were designated Mark III, Mark IV and Mark V respectively. Performance test equipment had to be built or modified to make the required tests. It was particularly important to achieve the power levels necessary to simulate those of real applications.

The tests which have been performed were designed to evaluate the suitability of MOLICELs for electric vehicle traction. To specify these tests, it was necessary to develop some understanding of the demands of this particular application and at the same time to acquire comparative data from other possible EV battery systems.

Finally, the work addressed the question of safer operation through thermal management. Fortunately the BC cell proved to have certain experimental advantages. For example, in order to test the theoretical heat flow model, it was necessary to implant thermocouples within the active cell materials and to make multiple feedthrough connections on the cell can. All this was possible on the BC cell whilst in no way preventing the normal cell operation.

2. HARDWARE DEVELOPMENT

The actual hardware development was carried out independently of the project. Accordingly this report contains only a brief superficial account of the activity.

Figure 1 shows a cross section of the Mark III BC cell. The can hardware is stainless steel and is comprised of a base, cylindrical section and header (top). The jelly roll is comprised of one lithium metal foil, two separators and two cathodes (MoS_2 on aluminum). The foils are approximately 12.5 cm wide x 670 cm long. The mandrel upon which the foils are wound is connected to the can by heat sink plates top and bottom which have a tight fit within the cylinder. Appropriate insulator discs prevent short circuits at these discs.

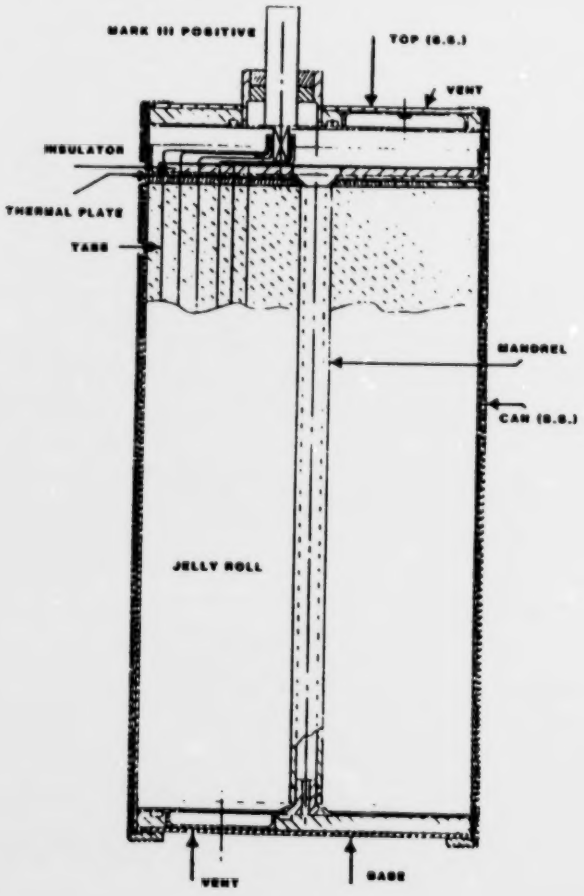

Figure 1: Cross section of BC cell (Mark III)

The anode and cathode foils each have six current collector tabs along their length. These tabs are brought into the header area and are joined by spot welding to corresponding tabs attached to the positive and negative posts. Figure 2 shows the arrangement of these posts on the header as well as the individual post detail on the Mark IV and V designs. The can is negative and is attached to the tabs from the lithium anode. The design of this post is straight forward. The positive post which is attached to the cathode tab is more complex. It contains a glass/metal seal in which the centre element is cored with copper. The copper protrudes as shown to provide intercell connection through a specially designed crimped pig-tail assembly. This unit was designed and built by Moli Energy.

Pressure relief vents are also located in both the top and bottom of the can. These vent discs are actually the bottoms of C cells which have been coined in the standard way to relieve at 400 psi.

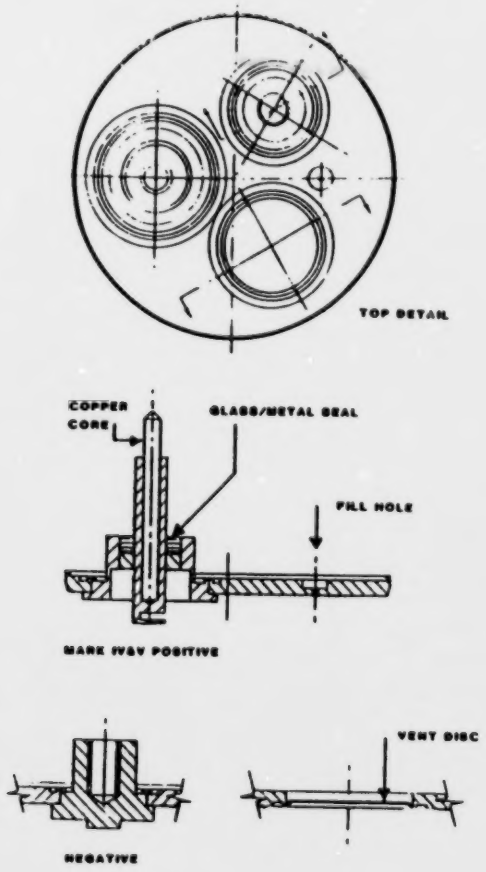

Figure 2: Header and base showing negative and positive posts as well as vents (Mark IV and V design).

The cell is wound and assembled dry. The final step is to pressure wet the active material and separator with an electrolyte comprised of a lithium salt dissolved in a mixture of aprotic solvents. This is known as the MOLI type II electrolyte and was used in all the cells built for the present study. After filling, excess electrolyte is removed and the can closed by welding a steel ball into the fill hole in the header.

The hardware of the header and the method of tabbing and of tab attachment were very different from the earlier designs used in Mark I and Mark II cells. The principle differences between the three cell types used here are as follows:

Mark III - Non-cored positive. Assembly by attachment of positive tabs to the post and negative to the can. Design rejected because of assembly difficulty and excessive resistive losses in hardware.

Mark IV - Cored positive. Assembly by tab-to-tab spot welding and spatial positioning jig allowing easy access and reliable closure in final T.I.G. welding steps.

Mark V - A minor revision of above with modified tab and insulator configurations at the foils.

Table 1 gives a breakdown of the system resistive components for three cell types. This shows that very significant reductions in hardware resistance have been achieved and it was therefore anticipated that the power capabilities would be realized. It remained to establish what the power capabilities were and how they related to specific applications requirements.

Unfortunately, this redesign exercise was not completed without penalty. The gross weight of the BC cell rose from 1000 g to 1250 g. Part of this came from the use of 0.125" steel plate for the base and the header in order to stiffen these members to provide for easier multi-cell battery assembly and safer cell interconnections. Thinner metal generally results in bulging and deformation which are aesthetically and mechanically unattractive.

Table 2 gives a full list of cells made, their designs and their ultimate disposition. A small number of cells were completely assembled but were never put to test because of failure to pass acceptance criteria usually as a result of an internal short circuit.

TABLE 1 - BC CELL RESISTIVE COMPONENTS

CATHODE	mΩ
Foil to .005" Al. Tab	1
Tab	0.4
Tab to .010" Ni	0.05
.010" Ni Tab	1.1
Tabs to Post	0.1
Post	0.15
ANODE	
Foil to .001" Ni	0.75
Tab	1.4
Tab to .010" Ni	0.01
.010" Ni Tab	1.1
Tabs to Post	0.12
Post	0.30
TOTAL EFFECTIVE HARDWARE RESISTANCE (MARK IV)	1.6 mΩ
MARK II HARDWARE	4.0 mΩ
MARK III HARDWARE	2.7 mΩ
JELLY ROLL CALCULATED BY SCALING C CELL DATA	2.9 mΩ
MARK V TOTAL MEASURE	3.8-4.8 mΩ
EXPECTED	4.5 mΩ

TABLE 2 - BC CELLS FABRICATED AND TESTED

Cell Number	Design (Mark)	Tests Performed*
85 0819-001	III	C, S (10;21;0/3), P (10;21;0/3), T.
0827-001	III	C
0829-001	III	C
0829-002	III	C
0919-001	IV	C, R(10,50,100;21;0/3) R(100;0,-20;0/3) P (20,50,100;21;0/3) P(100;0,-20;0/3) S(100;21;0/3)
1003-001	IV	C, R(10;21;1/3), P(10;21;1/3)
1119-001	IV	H
1119-002	IV	H
1213-001	IV	C, R(10;21;2/3), R(10;-20;0/3), P(10;21;2/3), P(10;-20;0/3).
86 0107-001	V	disassembled
0110-001	V	C, R(10,50;21;1/3), R(50;21;2/3), P(10,50;21;1/3), P(50;21;2/3).
0113-001	V	C, BP
0120-001	V	C, S(10;21;0/3)
0121-001	V	C, R(10;0;0/3), P(10;0;0/3), D
0123-001	V	C, BP
0123-002	V	C, R(10;-20;0/3), P(10;-20;0/3)
0124-001	V	C, BP
0127-001	V	C, BP
0129-001	V	C, BP
0130-001	V	C, BP
0220-001	V	H
0220-002	V	H

TABLE 2 - BC CELLS FABRICATED AND TESTED (con't)

Cell Number	Design (Mark)	Tests Performed*
85 0823-001	III	A
0828-001	III	A
0924-002	IV	A
0925-001	IV	A
0926-001	IV	A
0930-001	IV	A
1001-001	IV	A
1002-001	IV	A
1004-001	IV	A
1007-001	IV	A
1008-001	IV	A
1009-001	IV	A
1010-001	IV	A
1105-001	IV	A
1105-101	IV	A
1127-001	IV	A
1210-001	IV	A
86 0109-001	V	A
0205-001	V	A

*** Test Coding:**

Description	Code
Capacity vs. cycle number	C
Capacity vs. temperature	T
Capacity vs. current	S
Peak power vs. temperature	P
Peak power vs. depth of discharge	P
Power vs. energy	R
Duty cycle	D
Safety and abuse testing	A
Thermal analysis	H
Battery pack	BP

All tests may include following sub-sets:

- cycle number
- temperature
- depth of discharge

The code subsets are therefore defined as:

CODE (cycle number; temperature ^{o}C; depth of discharge in thirds)

All cycles are 2.4 to 1.1 volts. Unless specified, the temperature is 21^{o}C with 10A discharge. The recharge is always 5A.

3. PERFORMANCE TESTS AND EQUIPMENT

Table 3 lists the performance tests and the equipment upon which they were done.

TABLE 3 - TESTS PERFORMED AND EQUIPMENT USED

Code	Test	Equipment
3.1.1 3.1.2 3.1.3	Capacity vs. cycle number Capacity vs. temperature Capacity vs. current	Cycling system
3.2.1 3.2.2	Peak power vs. depth of discharge Peak power vs. temperature	Peak power tester
3.3	Power vs. energy	Constant power discharge system
3.4	Duty cycle	Duty cycler

The nature and functions of the four pieces of test equipment are described briefly and circuit block diagrams are given.

3.1 Cycling System

This system is the basis of all standard performance tests on rechargeable batteries. The basic functions of the Moli Energy system are shown in Figure 3.

The system consists of a number of analog current controllers, (chargers) connected to a microprocessor controller which communicates to a main computer with a hard disk for mass storage of data. The charger controls the current in the battery to the setpoint selected by the microprocessor. It also has an instrumentation amplifier which sends the battery voltage signal to the microprocessor.

The microprocessor controls all the chargers parameters; battery voltage switchpoints, charger output currents, test sequences, stores voltage readings and sends data to the main computer for storage. The test sequences are setup on the main computer which relays the information to the microprocessor controller. The allowable tests are; constant current charge and discharge, and signature curve (capacity vs. current).

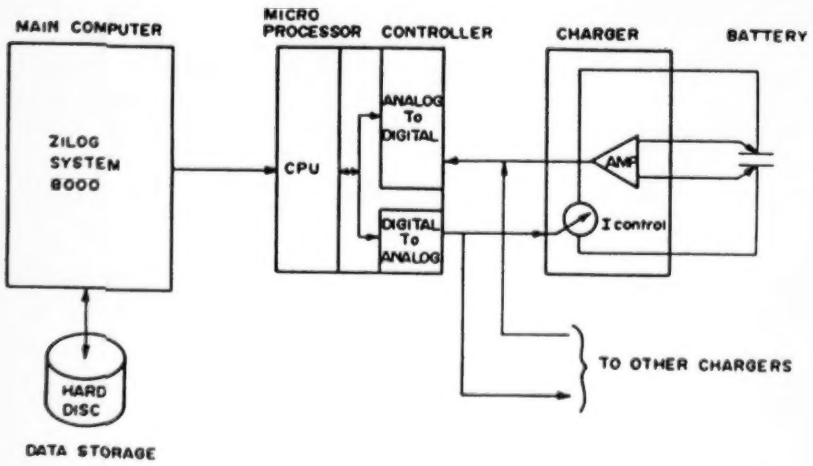

Figure 3: Block diagram of charging system

The capacity vs. current test is frequently used to compare the discharge rate capabilities of different cells and different cell designs. Its value as a true applications design tool is limited by the fact that the discharge is done at constant current and not at constant power. For this reason the present series of BC cell performance tests included both constant current and constant power discharges. A constant current discharge test tends to be a lengthy procedure because to build-up the required data the cell has to be discharged at one current, recharged, then discharged at another current and so on until the required current range has been covered. With a C/10 charge rate this ties up equipment for several days. The process is accelerated to produce what is called a signature curve. This has been shown to be a totally acceptable substitute for a longer and undoubtedly more precise test procedure. In the signature curve test, a cell is discharged at successively lower currents to the desired cut-off voltage. In the case of BC cells, the currents are 50, 25, 10, 5 and 2 amps with a 30 minute standby between each discharge. The capacity at a given current is taken to be the sum of the capacity obtained at the particular current plus all the capacities obtained at all the previous higher currents. The output of the test is given in the form of a plot of capacity vs. current.

Cells undergoing tests are maintained in a constant temperature environment. This is either an incubator with forced air circulation or an aluminum block through which a fluid circulates from a constant temperature system. Tests were performed on BC cells at -20°C, 0°C and 21°C.

A battery pack of six cells was also cycled using this equipment.

3.2 Peak Power Tester

The tester is shown in Figure 4. It is simply a method of applying and measuring various high power discharges for short periods. It should be noted that the range resistors R_1 to R_5 have very low values and are actually copper bars to carry the high currents involved.

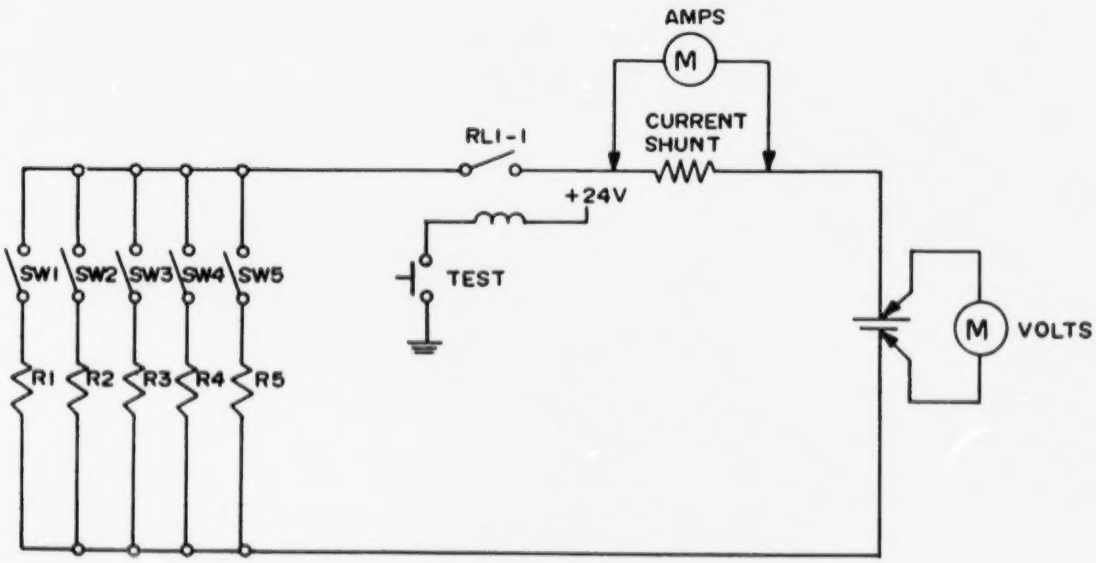

R1 - 32 mΩ
R2 - 16 mΩ
R3 - 8 mΩ
R4 - 4 mΩ
R5 - 2 mΩ

PRESS TEST BUTTON. TAKE CURRENT AND VOLTAGE READINGS AFTER 5 SECONDS. RELEASE BUTTON.

Figure 4: Block diagram of peak power tester

The battery voltage and the current are monitored with chart recorders. The current shunt is a 0.667 milliohm resistor. A combination of switches are selected to give the desired load resistance. The test button is depressed, closing the relay allowing current to flow through the current shunt and through the selected load resistors. After five seconds the button is released and the measurements are read off the chart recorders.

From a range of currents I, the internal cell resistance R is determined using the expression

$$R = \frac{V_o - V_1}{I}$$

where V_o is the open circuit voltage and V_1 is the voltage under load.

The peak power, W (peak), occurs when the internal and external circuit resistors are equal. Half the voltage drop occurs internally and half occurs externally.

$$\text{Since } W = VI = V^2/R$$

$$\text{Then } W \text{ (peak)} = \frac{V_0^2}{4R}$$

If the lower voltage cut-off is set at 1.1 volts then I max. is given by:

$$I \text{ max.} = \frac{(V_1 - 1.1)}{R}$$

The power at this point is therefore $\frac{(V_1 - 1.1)}{R} \times 1.1$

All plots involving peak power were obtained with strict application of the lower voltage cut-off. The peak power for a portion of the discharge is therefore said to be voltage limited. It must be recognized that this is an artificially imposed condition.

3.3 Constant Power Discharge System

This system is often referred to a sustained power discharge. The apparatus is based around an electronically controlled variable load as shown in Figure 5.

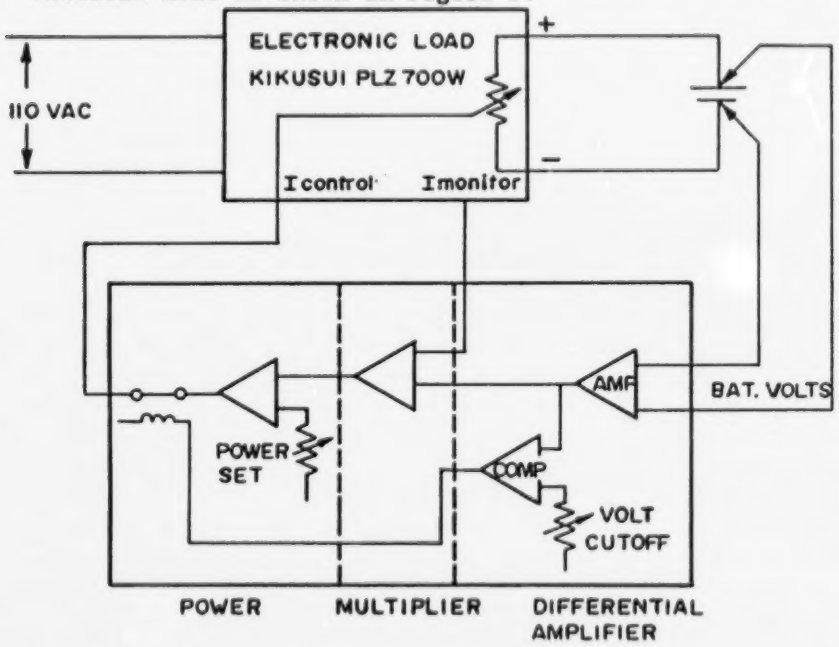

Figure 5: Block diagram of constant power tester

The power setting and battery cut-off voltage are adjusted before starting the test. The battery voltage is monitored with a chart recorder and also fed into an instrumentation amplifier. The output of the instrumentation amplifier is compared with the battery voltage cut-off point. If the battery voltage goes below the set voltage limit, the relay will open cutting off the current control voltage (Icontrol) to the electronic load. The battery voltage and current monitor voltage (Imonitor) are fed into the multiplier which gives a voltage output proportional to the power. This power signal is fed into a high gain amplifier which controls the current in the electronic load to make the power signal equal the power set voltage. The time for a power discharge is read off a chart recorder.

Thus the product of the power (W) and the recorded time (hours) gives the energy (W hr) of the discharge. If these data are plotted on log-log paper then a curve is obtained which is usually referred to as a Rogone curve. The Rogone curves are very useful for comparative purposes. In this case, the specific power vs. specific energy values are calculated by dividing power and energy by the battery/cell weight in kilograms. For very small cells one would be interested in volumetric comparisons and in this case the power and energy would be divided by the battery/cell volume in litres.

Quite frequently the Rogone relationships are plotted in a log-linear fashion with log specific power vs. specific energy. These plots are straight lines and they also form a useful basis of comparison.

From a design engineering point of view the Rogone plots do not give directly the most sought after information which is usually the time to discharge at a particular current. This is best obtained using the Peukert relationship.

$$\log t = \log C - n \log I$$

C and n are constants, t is the time to discharge, I is the current. A log-log plot of I vs. t should be linear but in practice this is not the case at high currents. The relationship is however useful and data from sustained power discharge are presented here in the form of Peukert plots just for completeness.

3.4 Duty Cycler

Figure 6 gives the block diagram of the duty cycler.

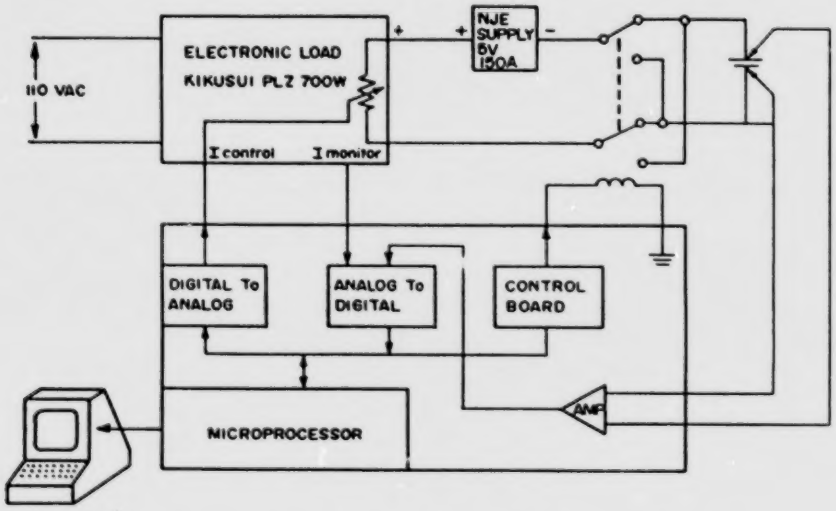

Figure 6: Block diagram of duty cycler

The relay connected to the battery is used for current direction control, as the unit can charge or discharge a battery. The relay is shown in the charge position. The 5 volt, 150 amp power supply is used to drive current through the battery in either direction. The battery voltage is fed to an instrumentation amplifier and then converted to a digital value for the microprocessor to read. The microprocessor takes the battery voltage reading and the power which the operator has selected and calculates the needed current. The microprocessor then outputs this digital current value to a digital to analog converter. This signal is applied to the electronic load to control the current in the battery (Icontrol). This power adjustment occurs 20 times a second. The microprocessor keeps track of the charge and discharge times and the upper and lower voltage setpoints.

The duty cycle is shown schematically in Figure 7. The peak power, base power, peak time and base time are all independently adjustable. The ranges available are limited by the conditions stated but they more than adequately cover the requirements to simulate electric vehicle applications.

In an actual cycle test the required parameters are established and entered into the microprocessor. The fully charged cell is then discharged according to the cycle regime and the total time to voltage cut-off is measured. Since the average speed over the simulated cycle is known then the vehicle range can be determined. Note that the cycle stops when the cell is no longer able to execute all the cycle requirements. The system does not compromise to a "best-effort" performance.

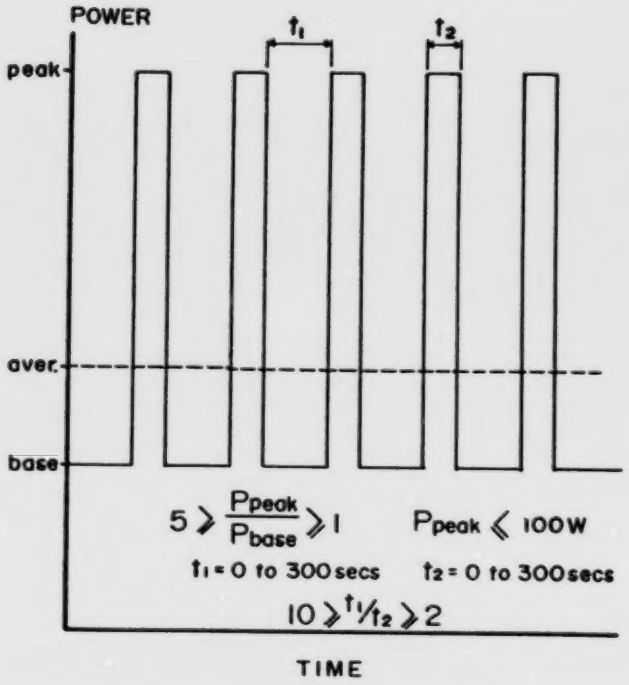

Figure 7: Duty cycle showing ranges of the variables

4. PERFORMANCE TEST RESULTS

4.1.1 Capacity vs. Cycle Number

Cycling was done between 2.4 and 1.1 volts with a charge current of 5A and a discharge of 10A. The capacity undergoes an initial fade but reaches a plateau at about cycle 10. The plateau value varies between 41 and 49 Ah. A typical plot of capacity vs. cycle number is shown in Figure 8. No attempt was made in the course of this present program to demonstrate long cycle life. The arguments of Section 1.2 apply to the issue of cycle life which is already demonstrated on AA size cells. Cycle life performance of BC cells can be expected with current technology to compare directly to AA cells for which present data show at 90% DOD, a life of 400 cycles before the capacity reaches 80% of the nominal rated value. A fully engineered BC cell could therefore be expected to reach a capacity of 35 Ah after 400 cycles.

A battery pack comprised of six BC cells in series was cycled at charge and discharge rates identical to these used for single cells. Figure 9 shows a plot of voltage vs. time for a 10A discharge at cycle 5. This is representative of a normal MOLICEL voltage profile. Table 4 gives individual voltages

after 40 cycles. There is considerable imbalance in this pack which is not normal for battery packs comprised of MOLICELs of AA size. This reflects the fact that the BC cell is not a mature engineering design and that its performance characteristics are not completely reproducible on account of the manual assembly.

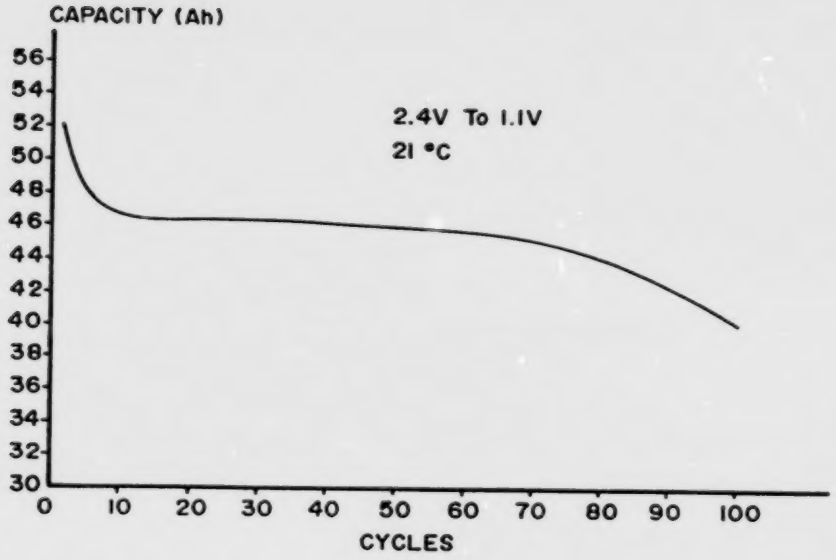

Figure 8: Plot of capacity vs. cycle number

TABLE 4 - BATTERY PACK VOLTAGES AFTER 40 CYCLES

Cell Number	Open Circuit Voltage (Fully Charged) volts	Under Load Voltage (10A Discharge) volts
1	2.233	2.142
2	2.431	2.350
3	2.003	1.928
4	1.965	1.887
5	2.060	1.965
6	2.034	1.952

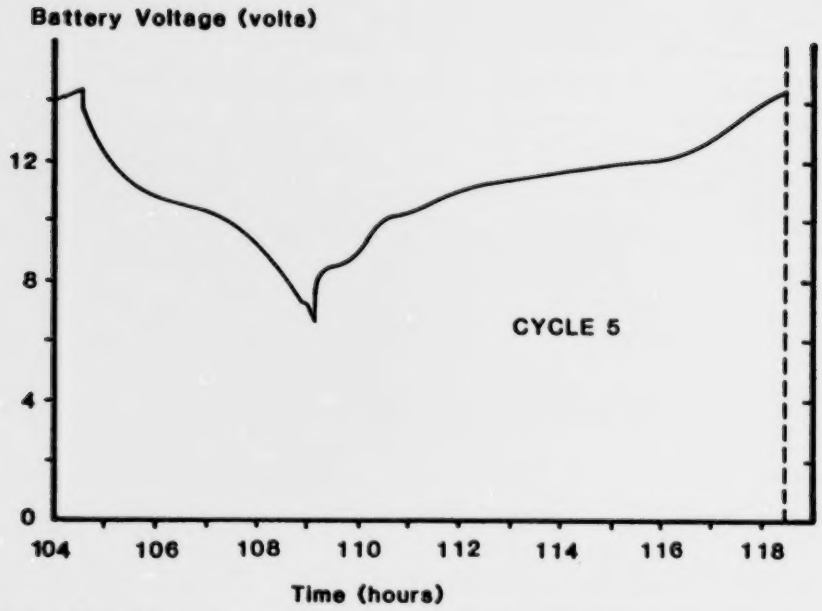

Figure 9: Plot of voltage vs. time for a single cycle of a pack of six BC cells. Charge at 5A. Discharge at 10A

4.1.2 Capacity vs. Temperature

The capacity of any cell is dependent upon temperature. Generally the low temperature penalty is not severe. The BC MOLICEL suffers a 25% loss of capacity between +20°C and -20°C as shown on Figure 10. In the electric vehicle applications for which this cell is developed, thermal management is required for power and safety considerations. Under these circumstances the issue of capacity loss with decreasing temperature is of little consequence.

4.1.3 Capacity vs. Current

As mentioned earlier, this test is particularly valuable as a comparative tool. The discharge is made at constant current and therefore at ever decreasing power levels. The measurement was used here to evaluate design improvements made between Mark III and Mark IV cells. As shown in Figure 11, the Mark IV cells have a higher capacity for a given current than the Mark III cells. This is due entirely to the improvements made in the current carrying hardware. In particular, the terminal post design and the method of internal tab attachment resulted in appreciable reductions in the resistive losses in these components. It is not too meaningful to compare these data with those of Mark I and Mark II cells which were cycled over different voltage limits (2.4 to 1.3 volts as compared with the present 2.4 to 1.1 volts).

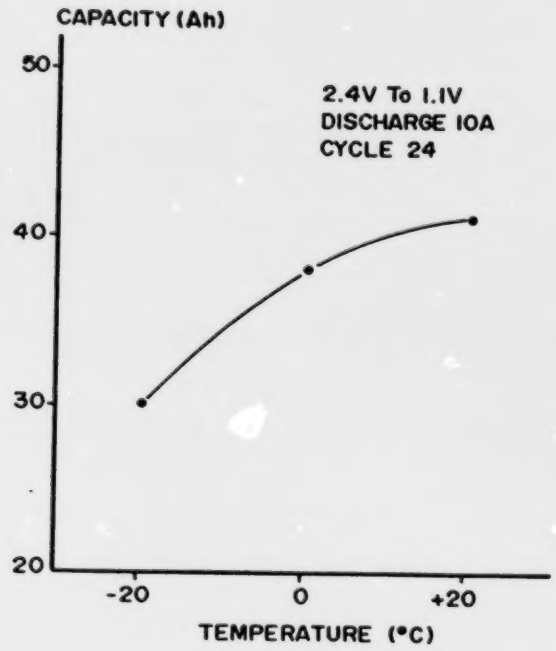

Figure 10: Plot of capacity vs. temperature

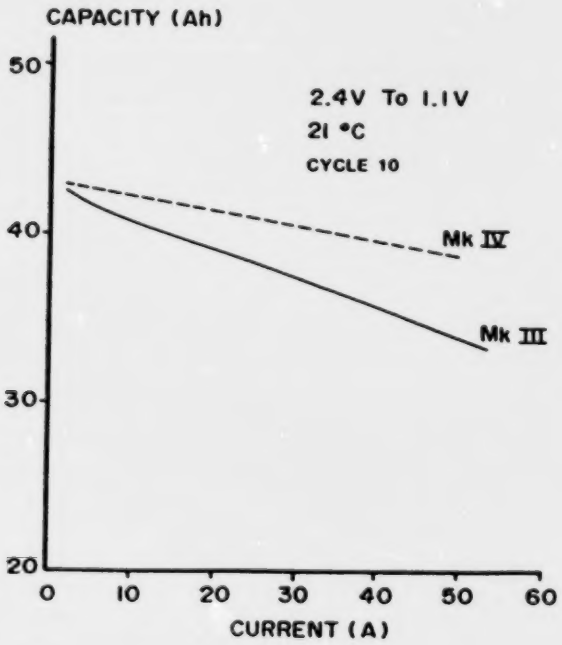

Figure 11: Plot of capacity vs. current for two cell designs

4.2.1 Peak Power vs. Depth-of-Discharge

This test provides particularly valuable design data. In Section 7 there is an explanation of its use in electric vehicle applications. A detailed description of how these data were obtained is given in 3.2. The purpose of this is to ensure that the reader can make meaningful comparison with data obtained from elsewhere about possible competitive cells. In Section 7 some comparative data are presented. These are to the best of our knowledge fair and meaningful comparisons. It should be recalled that the power capability of the MOLICEL is certainly not zero at 100% depth-of-discharge. The latter is defined as the point at which the cell voltage reaches 1.1 volts. Since this is chosen as the end of discharge then it is correct to assign a power capability of zero watts at this point. This is not a measured point but simply a defined condition.

Figure 12 shows the peak power results. The dotted section is an extrapolation. An examination of other peak power data confirms that this is the usual method of interpretation and presentation of test results.

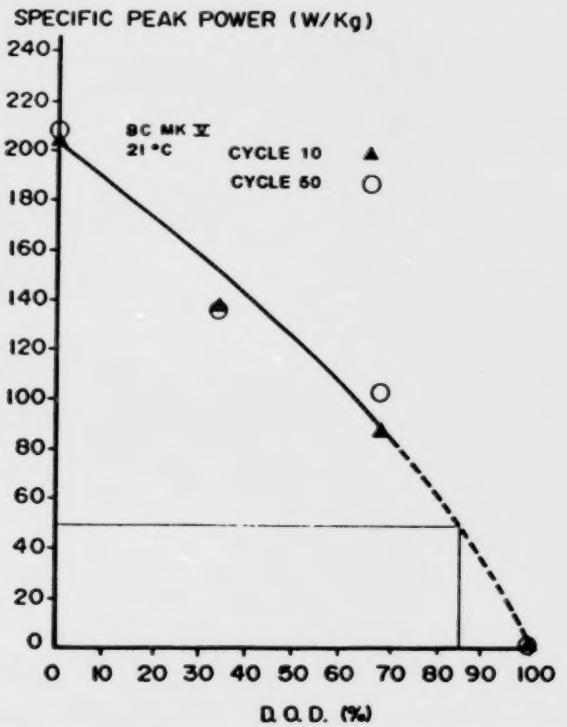

Figure 12: Plot of specific peak power vs. depth-of-discharge. Line shows usable D.O.D. of 85% at 47 W/Kg. See section 7.1

4.2.2 Peak Power vs. Temperature

Figure 13 shows the results of data for peak power at three temperatures. These results are for fully charged cells. The error bar at -20°C reflects a situation which is incompletely understood. The data indicate that the cell impedance at -20°C is not constant. The effect is unlikely to be caused by internal heating because the test pulse duration was 5 seconds and this was followed by a minimum wait of 15 minutes for temperature equilibration.

It is somewhat surprising how much decrease in specific peak power occurs in the cycle 100 tests. The effect is a result of a rise in the cell internal impedance. Very much larger useful cycle life is being obtained with fully engineered AA size cells. There is no fundamental impediment to achieving similar results on BC cells.

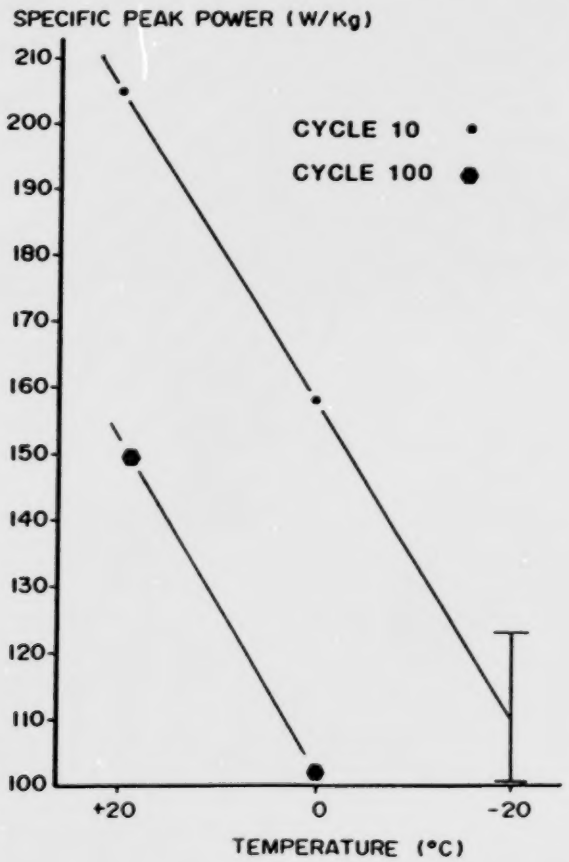

Figure 13: Specific peak power vs. temperature showing the influence of cycle number

4.3 Power vs. Energy

The power vs. energy characteristics of any cell depend on the cycle number, depth-of-discharge and temperature. Data for BC cells are plotted in Figures 14 to 18.

The real significance of these results only becomes apparent when specific duty requirements are defined. However, in a qualitative sense, there are no surprises. The variations of power and energy with depth-of-discharge are fully consistent with the MOLICEL discharge voltage profile and with the data in Figure 12. The effect of temperature is also consistent with Figure 13 as well as with established MOLICEL performance characteristics. It should however be pointed out that Figures 14 to 18 cannot be generated reliably from standard published MOLICEL performance data. They do comprise a unique data set which is invaluable for battery design and applications analysis.

Figure 19 is a Peukert plot showing power vs. discharge time. Although this relationship should give a straight line log vs. log plot, there is a negative deviation from the relationship at high powers.

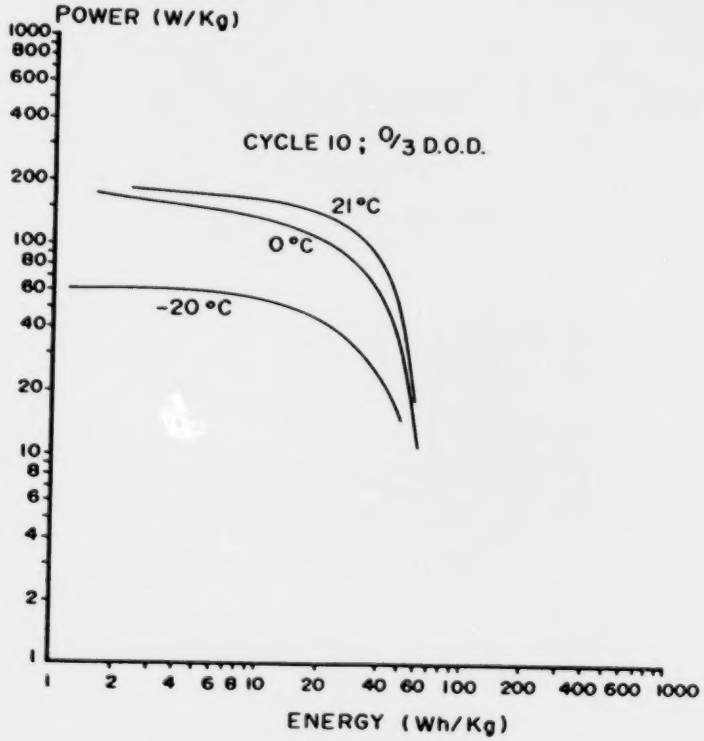

Figure 14A: Specific power vs. specific energy showing variation with temperature on cells at cycle 10

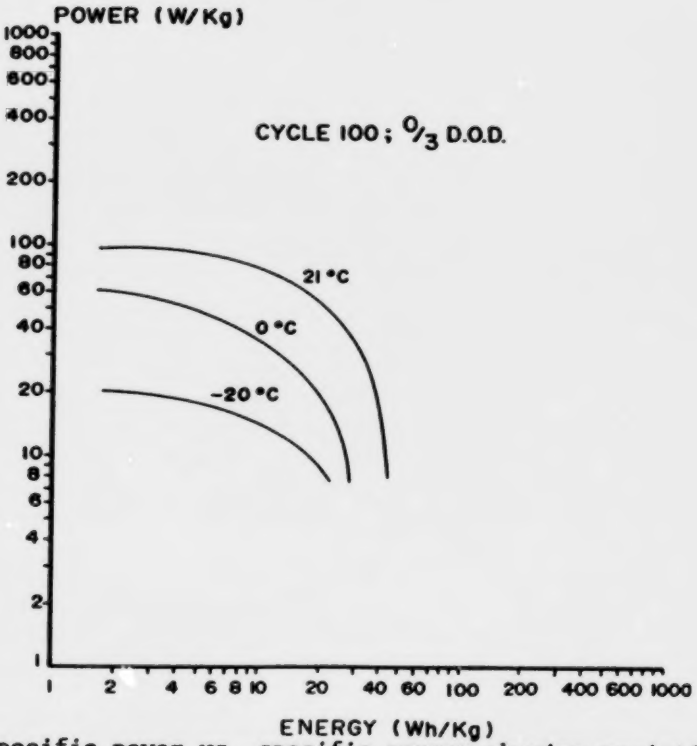

Figure 14B: Specific power vs. specific energy showing variation with temperature on cells at cycle 100

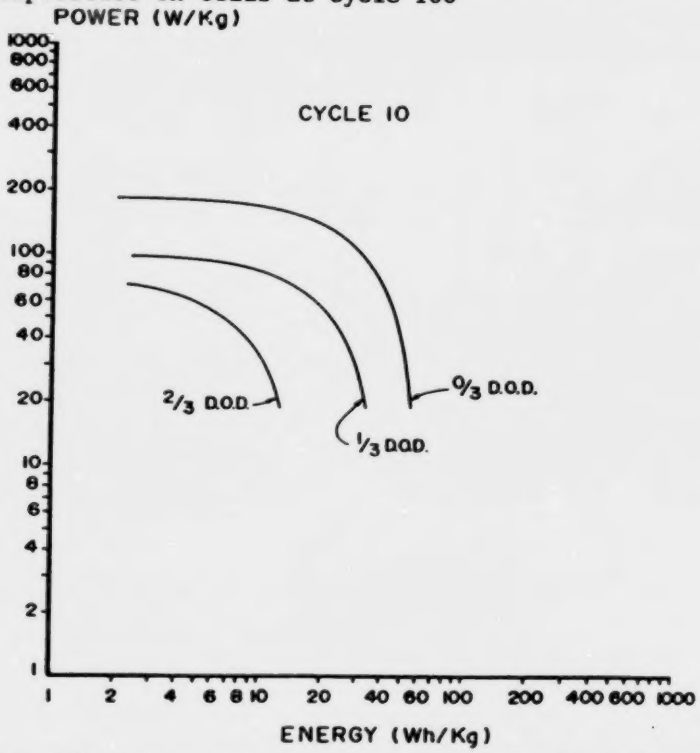

Figure 15: Specific power vs. specific energy showing effect of depth-of-discharge at cycle 10

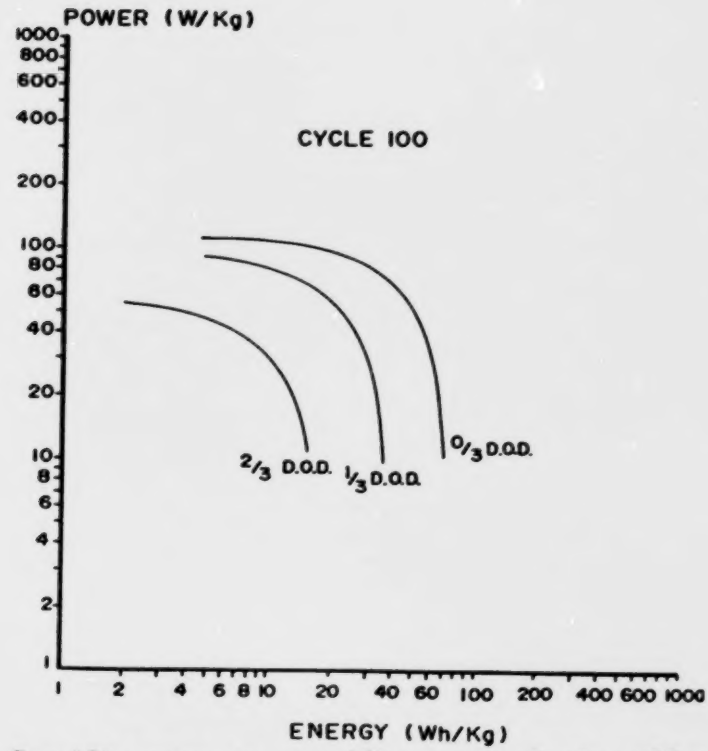

Figure 16: Specific power vs. specific energy showing effect of depth-of-discharge at cycle 100

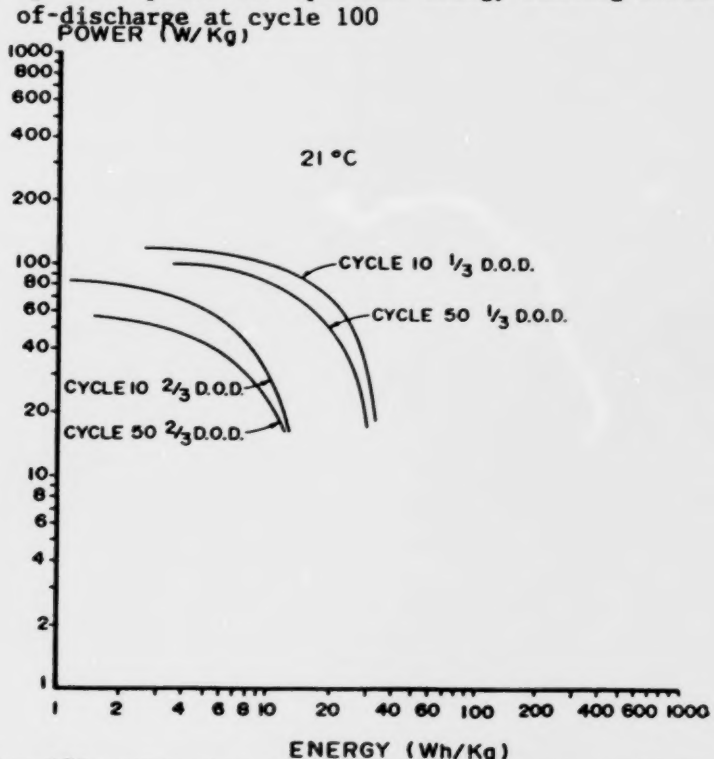

Figure 17: Specific power vs. specific energy showing effect of cycle number and depth-of-discharge

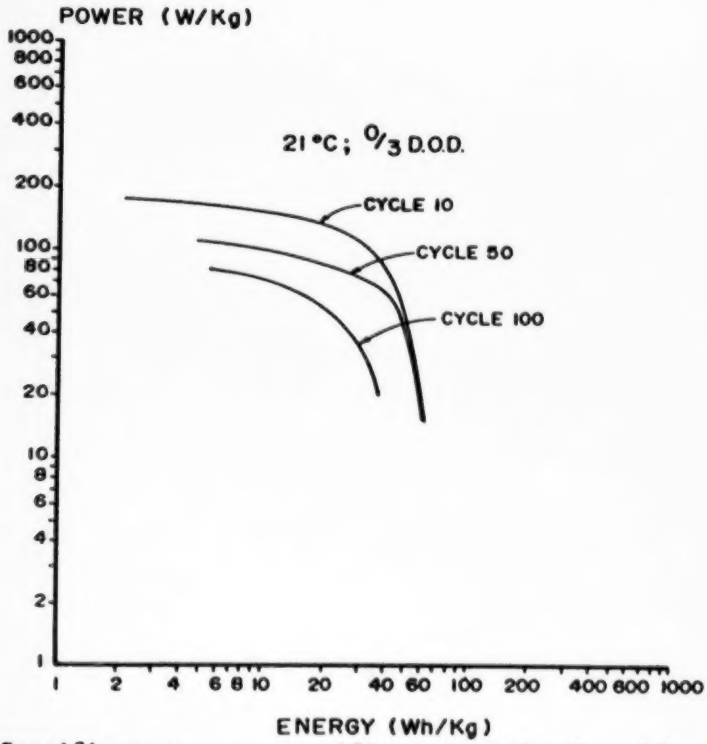

Figure 18: Specific power vs. specific energy showing effect of cycle number

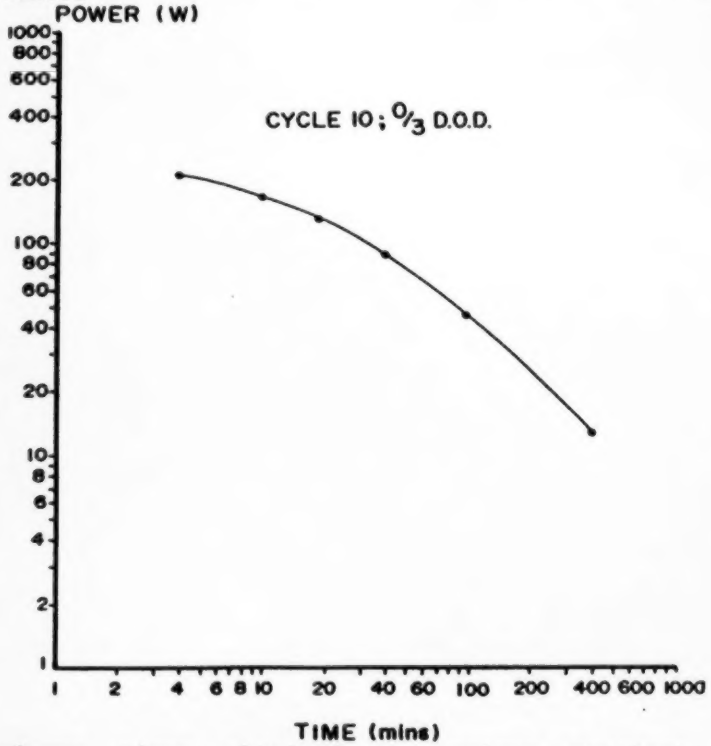

Figure 19: Discharge times obtained at various constant power discharge levels

4.4 Duty Cycle

Three duty cycle tests were made using a single Mark V cell which had completed 50 cycles. The cell was held at 21°C throughout the tests using a cooled aluminum heat sink block.

The cycles used are illustrated in Figure 20. They represent what might be required of a cell in an electric vehicle battery when the vehicle was repeatedly executing the SAE J227(a) schedules D & C (see Figure 21). Cycle 1 is a close approximation to schedule D and the total distance travelled is 1.6 km. Cycle 2 is the same as cycle 1 except that there is no rest period. Cycle 3 is an approximation of schedule C. It has a significantly lower peak power because the maximum speed is 48 km/hr vs. 72 in the schedule D. The total distance travelled is 0.487 km.

One variant of the tests was made. The duty cycle controller had provision to relax the 1.1 volt cut-off criteria for a fixed period - in this case set at 32 seconds. However, the cell voltage was never allowed to fall below 0.5 volts. This is equivalent to exceeding a "red line" condition on an automobile. Tests were conducted to determine the total distance "travelled" until the cell was discharged. It should be noted that a well cycled cell was used for this test. The results are given in Table 5.

TABLE 5 - DUTY CYCLE TESTS OF A SINGLE CELL

Duty Cycle	Special Conditions	Number of Cycles	Distance "Travelled" (km)
1	none	27	43
1	"red line"*	28	45
2	none	24	38
3	none	86	42
3	"red line"+	90	44

* set at 0.95 volts - the 140 A current limit of the system did not permit voltage settings below this for cycle 1

\+ set at 0.67 volts

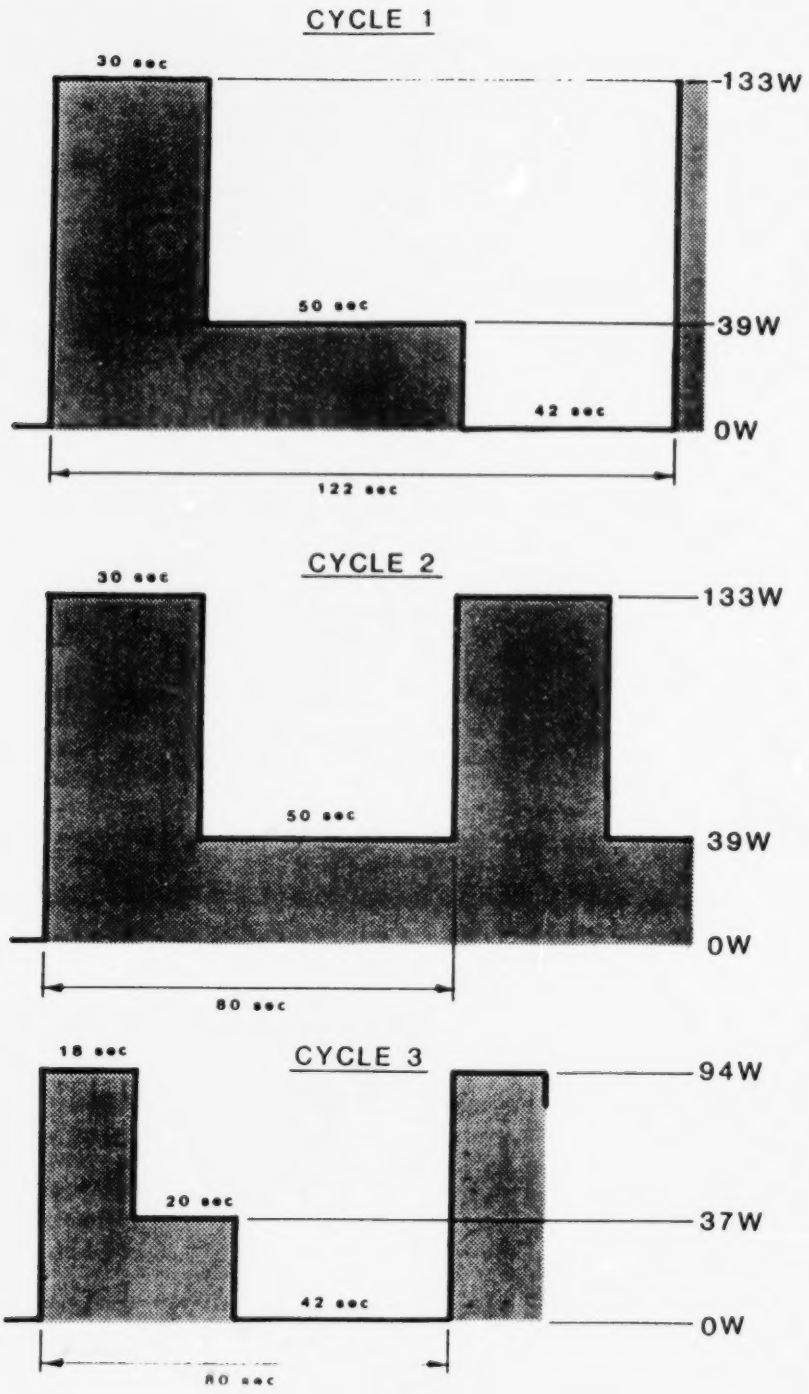

Figure 20: Experimental duty cycles representative of the SAE J227(a) schedules C and D. Cycle 1 is schedule D; cycle 2 is schedule D without a park period; cycle 3 is schedule C

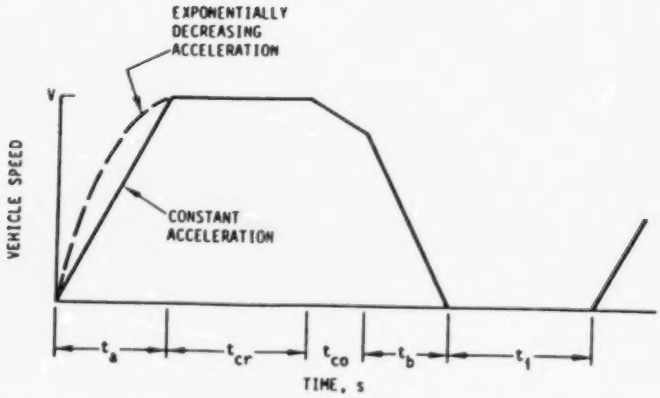

TEST PARAMETER	SAE SCHEDULE (all times in seconds) A	B	C	D
MAXIMUM SPEED (V). km/h	16±1.5	32±1.5	48±1.5	72±1.5
ACCELERATE TIME (t_a)	4±1	19±1	18±2	28±2
CRUISE TIME (t_{cr})	0	19±1	20±1	50±2
COAST TIME (t_{co})	2±1	4±1	8±1	10±1
BRAKE TIME (t_b)	3±1	5±1	9±1	9±1
IGLE TIME (t_i)	30±2	25±2	25±2	25±2
TOTAL TIME	39±2	72±2	80±2	122±2

Figure 21: SAE J227(a) duty cycles

The battery sizing and vehicle considerations leading to this comparison are to be regarded for the present as being artificial. Obviously the parameters were chosen to have some practical relevance and this will be apparent in Section 7. The most important conclusion is that even though very significantly different power requirements existed for cycles 1 and 3, there is no significant difference in the "range" achieved. Also the "red line" capability has little effect on the range and probably does not offer any real practical benefits. This reserve of energy is always present in the MOLICEL where the lower voltage limit is a selected operating parameter and is by no means the point at which the stored energy in the cell is zero. Wide excursions below the recommended limit can reduce the cycle life and should not be prolonged.

A further observation is that the removal of the "rest" period from the SAE J227(a) schedule D ie. our test cycle number 2 does carry some small penalty. In this case a 12% reduction in the "range" resulted. This is because of beneficial equilibration which occurs in the MOLICEL cathode on standing after a fairly heavy discharge pulse.

5. SAFETY TESTING

Safe operation of any cell requires predictable behavior under definable conditions. The critical parameters are:

- Design
- Quality control

The MOLICEL incorporates many safety related design features and AA and A size cells are manufactured to rigorous specifications. BC size cells incorporate some of these safety features but are hand made developmental products and do not have the engineering specifications or quality control of a production cell.

Operation of MOLICELs outside the limits defined in the technical specifications constitutes an abuse. However, these specifications cannot possibly cover all eventualities and in any case, misuse, either deliberately or accidentally can be anticipated at some time. Potential hazards are reduced by ensuring that the cells are very tolerant to abuse.

With AA size cells this condition can be achieved readily. Larger cells present an additional challenge. Not only do they contain more energy but their greater dimensions contribute to poorer thermal dissipation. If the internal temperature rises above the melting point of lithium (180°C) a strong exothermic reaction between the active materials will occur and high internal pressures are generated within the cell. Carefully designed vents relieve these high pressures and prevent an explosion.

It is convenient to define three envelopes of safety performance. These are illustrated in Figure 22. The envelopes are essentially distinguished by the nature of the cell performance under abuse. In the first case, the cell suffers no adverse effects. In the second case, the cell tolerates the abuse although it suffers some damage, including the possibility of a pressure relief venting. The cell is generally rendered inoperable as a result of abuse falling within this envelope. In the third case, the cell is destroyed. It usually burns and with large cells this can be quite a violent process. Because of the reliable operation of the safety vents, the MOLICEL does not explode under any abuse condition.

A matrix of tests has been applied to the BC cell to define its safety characteristics. These tests include the standard requirement of the U.S. Department of Transportation for lithium cell shipping under an exemption to the hazardous materials regulations, E-7052, to which Moli Energy is a party. They also include "Standard Tests for Lithium Batteries" UL 1642 as required by Underwriters Laboratories. In some cases the tests were modified. For example, the cells were not "preconditioned" with a high temperature storage prior to testing as is required by U.L. Also the drop and thermal shock tests as required by U.L. were omitted as well as the high altitude simulation and thermal storage required by D.O.T. The test

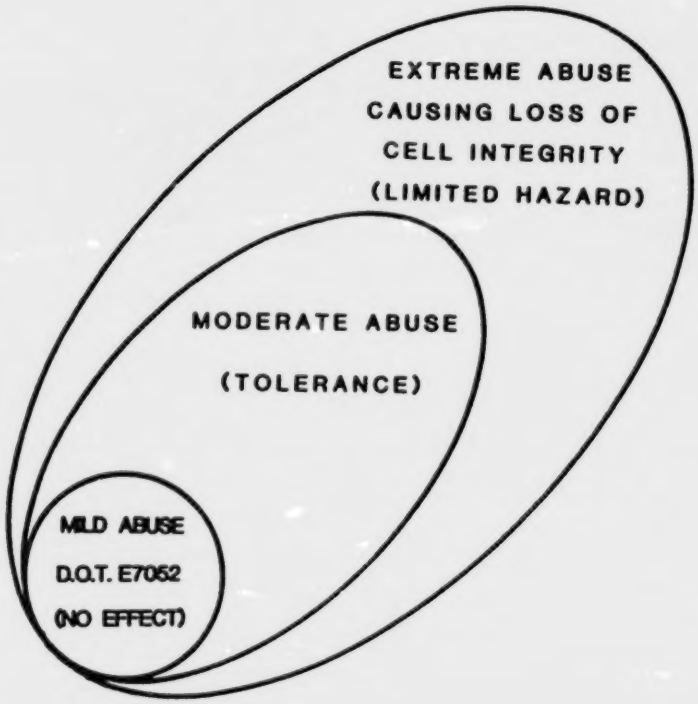

Figure 22: Illustration of envelopes of safety performance

matrix was as follows.

D.O.T. E-7052

- Vibration (10 to 55 Hz, 0.03 inch amplitude)
- Mechanical shock (175 G).

UL 1642

- Overheating
- Overcharge
- Forced Discharge
- Short Circuit
- Crush
- Incineration

Tests were conducted on fresh cells and on cycled cells. D.O.T. establishes simple fail/pass criteria. Cells subjected to the four defined tests (the present matrix omits high altitude simulation and thermal storage) are required to undergo no change in appearance, weight or voltage as a result of the test conditions. Underwriters Laboratories on the other hand has no such criteria for their tests although to receive acceptance generally requires that the cells tolerate the abuse and in no way contribute an aggravation of the hazard. The AA size MOLICEL does meet these requirements and has recently received U.L. "component recognition".

In order to complete this set of abuse tests, the use of diodes was investigated for protection against overcharge and against forced discharge. The details of these tests and their results are reported under the respective headings.

5.1 Vibration

The test is defined in Figure 23. The rate of change of frequency is 1 Hz per minute. The tests were conducted using two perpendicular vibration directions, one axial and the other radial. Cells were tested after one charge-discharge cycle and after 40 such cycles. Cell weights and voltages were unchanged in these tests. The mechanical integrity and appearance were not changed.

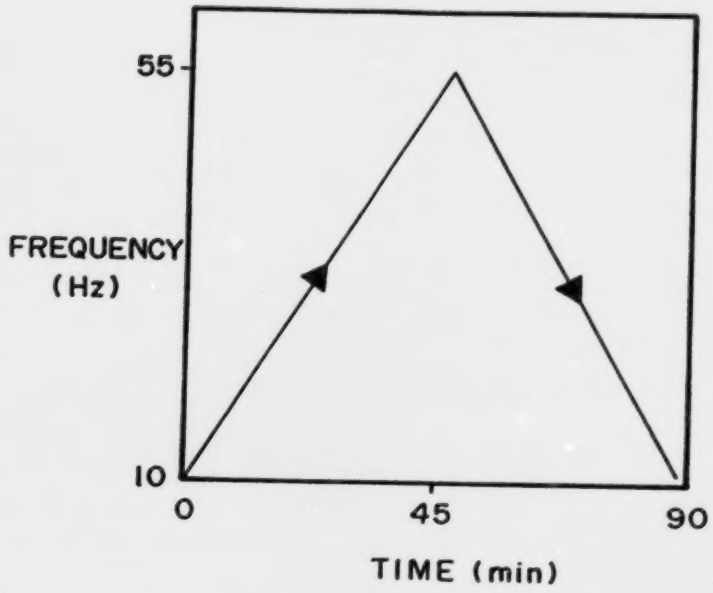

Figure 23: Schematic of vibration test under DOT-E-7052 requirements

5.2 Shock

The test involves an acceleration of >75 G over 3 milliseconds with a peak of 125 to 175 G. Actual recorded accelerometer data are shown in Figure 24. Again, the tests were conducted along mutually perpendicular axes. However, this time the acceleration was done in each of the two axial directions, ie. top to bottom and then bottom to top. Cells were tested after one standard charge-discharge cycle and after 40 such cycles. Cell weights and voltages were unchanged. The mechanical integrity and appearance were not changed.

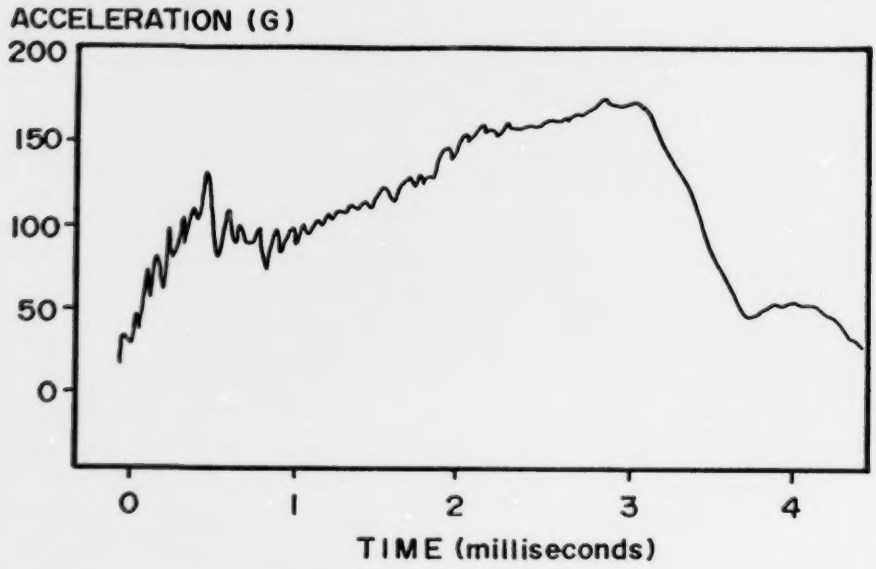

Figure 24: Actual accelerometer data from shock test under DOT-E-7052 requirements

5.3 Overheating

For these tests, cells were used after 1 charge-discharge cycle and after 40 such cycles. The cells were held in an electrically heated block and the temperature raised at 5°C per minute.

Figure 25 shows the results for a cell with 40 cycles. The

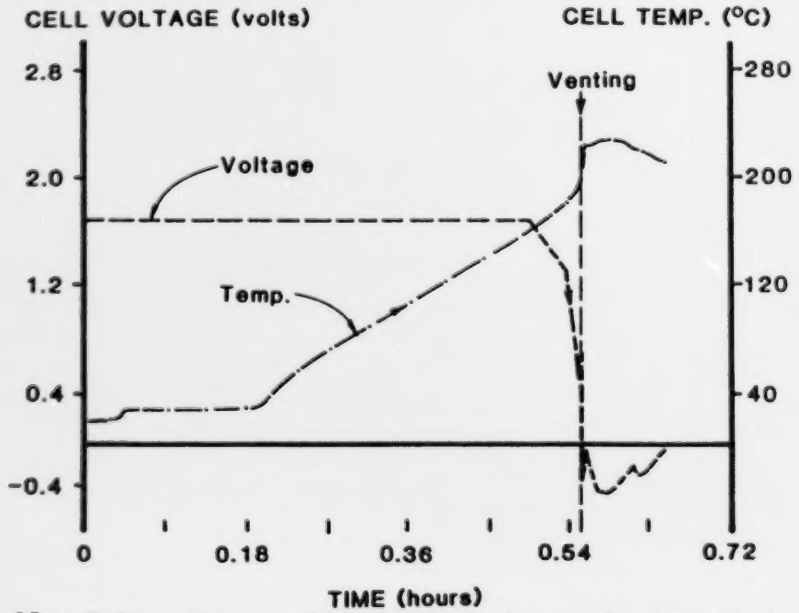

Figure 25: Cell voltage and temperature in overheating test

results on a fresh cell were very similar. In both cases, the cells exhibited vigorous venting and burning at a case temperature just above the melting point of lithium. AA size cells exhibit very similar behavior.

5.4 Overcharge

Cells at cycle 1 and at cycle 40 were fully charged at the start of these tests. Further charging was done at 5 amp (C/10 rate) taking the cell voltage above the normal 2.4 volt cut-off. Both cells failed with vigorous venting, accompanied by burning, after a substantial amount of excess charge had been passed. For the cycle 1 cell, this venting occurred after a further 80% of the nominal capacity had been passed. In a cycle 40 cell the venting occurred after 119% of overcharge. The effect is typified by the results of the latter test shown in Figure 26.

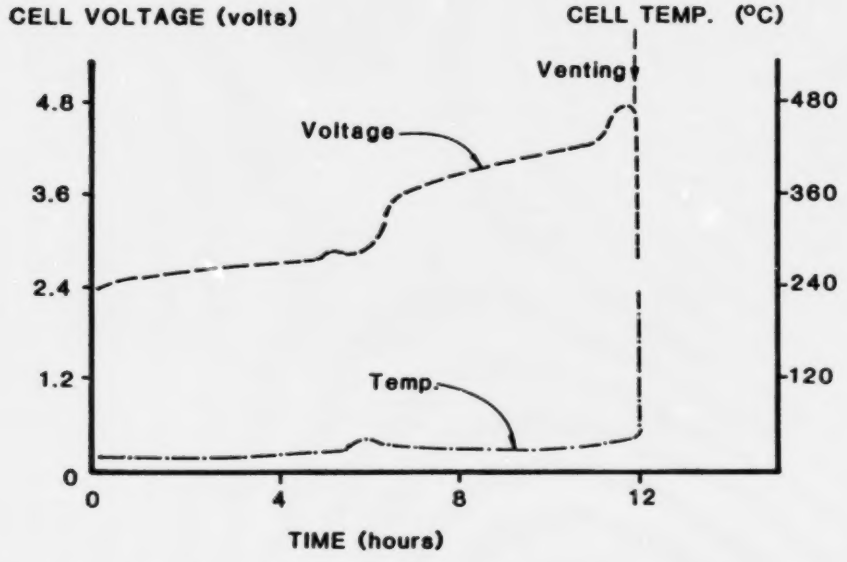

Figure 26: Overcharge of a cell at C/10 rate showing venting at 119% overcharge.

In order to protect against failure under conditions of overcharge the voltage can be limited with parallel diodes connected in the forward direction as in Figure 27. In this case 4 series diodes (IN3880) were necessary to limit the voltage to 4 volts. The test was repeated using this arrangement and the results plotted in Figure 28 show that protection against overcharge was achieved. The cell did not vent and the temperatures fell back to ambient after a brief excursion to 40°C. There are penalties with this diode arrangement in that some forward leakage will occur resulting in a discharge of the cell. The measured discharge current was 300 mA.

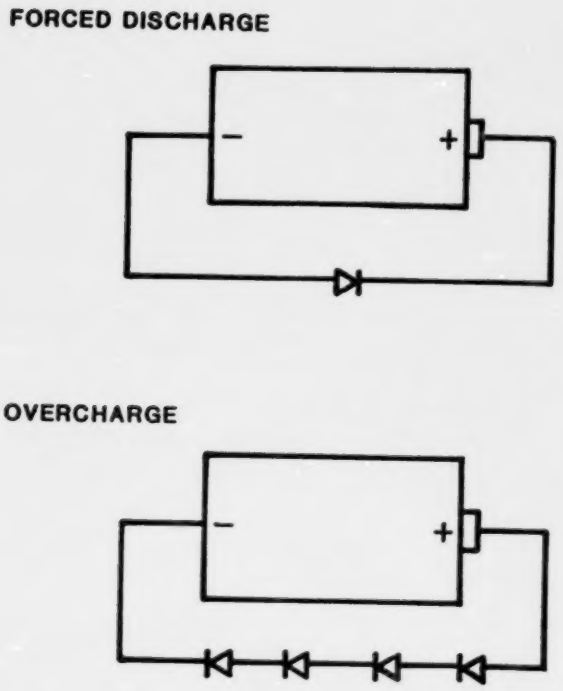

Figure 27: Diode protection of cells against overcharge and forced discharge

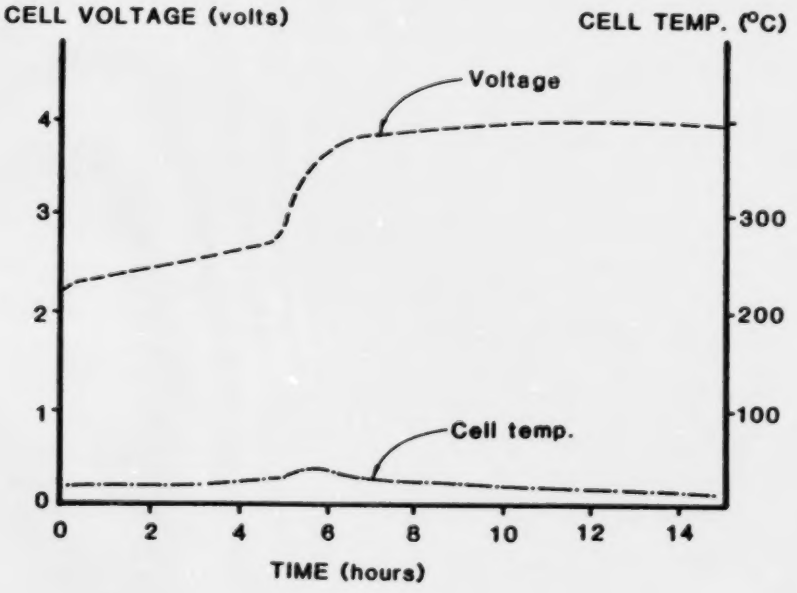

Figure 28: Overcharge with diode protection showing voltage cut-off as required and no significant temperature rise in the cell

5.5 Forced Discharge

Cells with 1 cycle and with 40 cycles were subjected to a discharge at 10 amp extending below the normal cut-off of 1.1 volts. In fact the cells were driven below 0 volts into a condition of voltage reversal. In the case of the fresh cell, after 211% of the capacity had been passed (10.56 hours) a vigorous venting occurred. The cycle 40 cell behaved similarly except that in this case, 156% of the capacity had been passed at the time of venting which occurred 7.78 hours into the test. Both cells were in fact driven below 0 volts before venting. The results for the cycle 40 cell are shown in Figure 29. The form of the graphs for the fresh cell were identical.

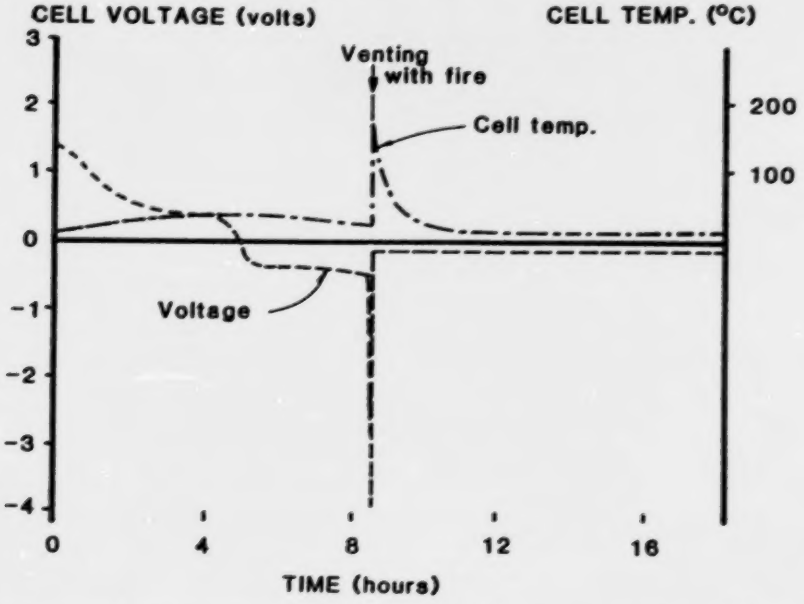

Figure 29: Forced discharge at C/5 rate showing venting after 156% overdischarge with the cell potential in reversal

Protection against forced discharge can be achieved using a diode connected in parallel to the cell but oriented in the reverse direction as in Figure 27. This protection is compatible with the forward connected diode arrangement used in overcharge protection and both systems can be applied simultaneously. The results of a forced discharge with diode protection are shown in Figure 30. No venting occurred.

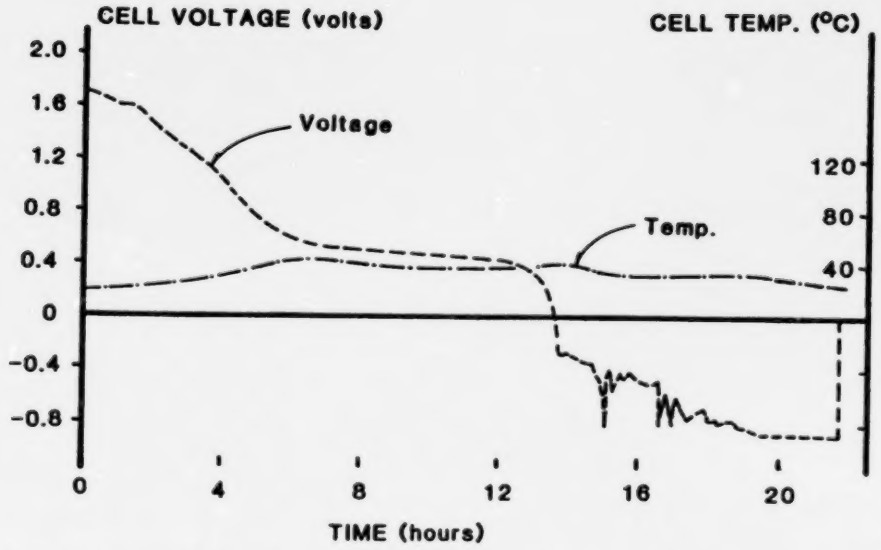

Figure 30: Forced discharge with diode protection showing cut-off at about -1 volt and no significant temperature rise

5.6 Short Circuit

Fresh cells and cells with 40 charge/discharge cycles were short circuited by connection to a circuit of 3.3 mΩ resistance. Tests were done with the cells in free air and with the cells in a cooled block held at 20°C. BC cells are generally intolerant of short circuit abuse. The high currents involved raise the internal temperature above the melting point of lithium and venting occurs with burning. In the case of a fresh cell held in a cooled heat sink block, the maximum temperature, as measured external to the can, was 129°C and venting was only a simple pressure relief without burning. A cycled cell (40 cycles) under the same conditions gave a higher short circuit current than fresh cells (275 A vs. 248 A). The temperature rose to over 300°C and the venting was accompanied by fire.

Figure 31 shows data plots from a short circuit of a fresh cell held in a heat sink at 21°C. The cell vented without fire after 19 minutes.

Figure 32 shows plots for a short circuit of a cycle 40 cell in still air. The cell vented with fire after 12 minutes.

It should be noted that venting in these cells occurs only after the short circuit has been sustained for fairly long times (>10 minutes). Also the short circuit currents are extremely high (>250 amperes) so that many externally applied shorts would be unlikely to sustain such currents. It is also encouraging to note the positive improvements obtained with effective external heat sinking. This issue is considered further in Section 6.

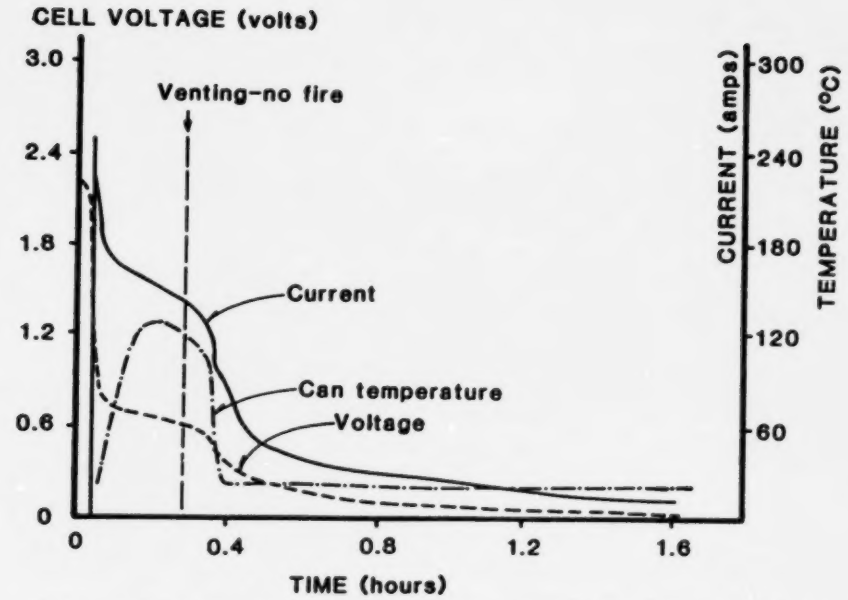

Figure 31: Short circuit of a fresh cell in a 21°C heat sink block showing the temperature at the top of the can as well as the cell voltage and current. Venting occurred without fire because of the temperature constraint from the heat sink.

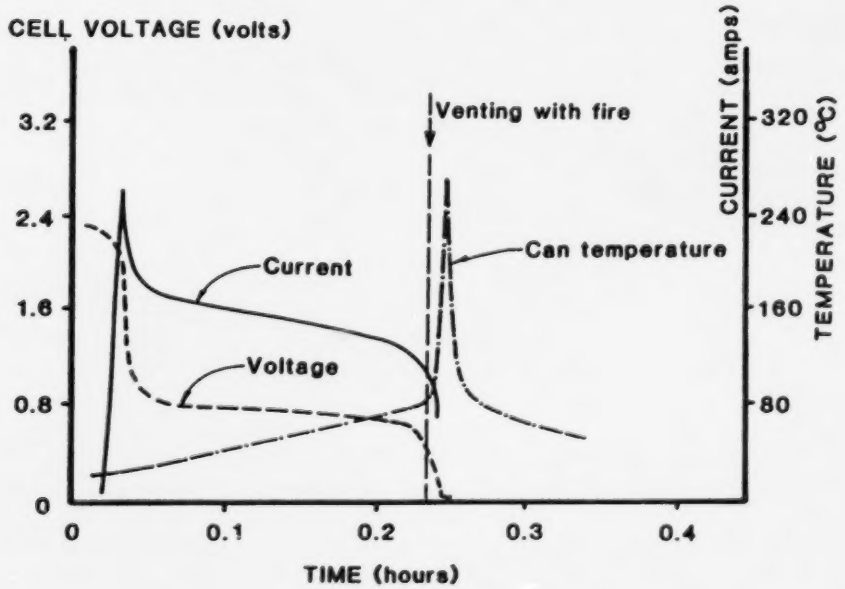

Figure 32: Short circuit of cell without heat sink. Venting occurred with fire and the can temperature reached 300°C. Short circuit current is 275 amperes

5.7 Crush

Cells were crushed between a flat plate and a 5/8" diameter bar carried on a hydraulic ram. Both fresh and cycled cells vent with strong burning when crushed to 25% of their original diameter. A force in excess of 3500 lbs. is required to produce this deformation.

5.8 Incineration

A large propane/air burner was used to engulf the cells in flame. Venting and strong burning occurred usually within 5 to 10 seconds.

As a modification of this test a cell was predischarged to zero volts then left connected to a 2Ω shunt for several weeks. Upon incineration, the cell vented but only mild burning of the electrolyte followed. The vigorous lithium reaction was not observed. This behavior is in sharp contrast to that experienced with primary lithium cells where reactivity would be high after such a discharge.

6. THERMAL ANALYSIS

6.1 Thermal Power

In order to collect accurate thermal data on a BC cell it would be necessary to construct a suitable calorimeter. This is not a simple task because of the size of the cell and the magnitude of the power dissipated. The present requirement would not justify the construction of such a calorimeter. Precise data are not needed. For this reason, it was decided to use calorimetric data obtained on C cells and to scale this to the BC size. The scaling factor used was based on the impedance ration of 20:1. Very little difference would result if this were to be replaced by the jelly roll volume ration of 21:1. Table 6 gives thermal power at various discharge currents.

TABLE 6 - THERMAL POWER AT VARIOUS DISCHARGE CURRENTS

Discharge Current (A)	Peak Thermal Power Output (W)
20	4.8
40	14.1
60	25.0
80	34.6

From the data the thermal power can be calculated for the various duty cycle steps of Figure 20.

The results are given in Table 7.

TABLE 7 - THERMAL POWER AT VARIOUS ELECTRICAL POWER LOADS

Discharge Power (W)	Peak Thermal Power (W)
39	12.3
94	37.7
133	55.0

The short circuit thermal power dissipation can be calculated using actual current/voltage data such as presented in Figure 32. These give a peak thermal power dissipation of ~375 W and an average power of 170 W.

These power values now define the task of thermal management of the BC cell to achieve safe operation under all conditions. Under conditions of normal operation, peak thermal power dissipation will not exceed 55 W. Under short circuit conditions a peak power of 375 W occurs briefly followed by an average power of ~170 W. Lower sustained power levels will result if the cell temperature is not allowed to rise. In this case the rising cell impedance serves to limit the circuit current.

6.2 Thermal Model

It was assumed that in the current standard MOLICEL design, all heat flow occurred radially through the jelly roll to the outer cylindrical can. If this is the case then a simple model can be used to predict the cooling of a BC cell.

The equation for radial flow in an infinite circular cylinder with no internal heat generation is given by

$$\frac{1}{r}\ \frac{\delta}{\delta r}\left[r\ \frac{\delta T}{\delta r}\right] = \frac{1}{k}\ \frac{\delta T}{\delta t}, \quad 0 < r <= b \qquad (1)$$

where $T(r,t)$ is the temperature dependent on the radius r and time t, b is the radius of the cylinder and

$$k = K/(\rho c) \qquad (2)$$

and is known as the (radial) thermal diffusivity. K is the radial thermal conductivity, ρ is the density, and c is the specific heat of the material of the cylinder.

If the boundary is kept at a fixed temperature Tb and the initial temperature To of the cylinder is uniform then the solution of equation (1) is given by

$$N = \frac{T - To}{Tb - To} = 1 - 2 \sum_{m=1}^{\infty} \frac{JO(Am.r/b)}{Am.J1(Am)} .e^{\{-(Am/b)^2 .k.t\}} \qquad (3)$$

where JO(x), J1(x) are Bessel functions of the first kind of order 0 and 1 respectively, and Am's are the positive roots of JO(x) = 0 (m = 1,2,3,....). N is the ideal normalized temperature, hence equation (3) is the equation of radial cooling in normalized form.

To test this model, a BC cell was instrumented with four thermocouples positioned along a radius in the mid-plane. The cell was mounted in a thermostated heat sink block at 21°C, equilibrated and then cooled by circulating the coolant at -9.6°C.

The thermocouple data were fitted to equation (3) and a value of the radial thermal conductivity was thus obtained. The fit of experimental data was excellent. It can thus be concluded that the radial cooling model is a very close approximation to the real cell condition. The jelly roll thermal conductivity obtained from the data fitting was 0.0048 W/cm°K.

6.3 Heat Flow Modification

6.3.1 Heat Sink Plates

Having established the validity of the radial cooling model it was decided to test the effect of the heat sink plates incorporated in all Mark III, IV and V cells used in this contract work. To do this a Mark IV cell was wound with radially disposed thermocouples as described earlier. This cell, unlike the previous test, was fitted with heat sink plates connecting the mandrel thermally to the top and bottom of the can. The cooling tests were repeated and the thermocouple data fitted to the radial cooling equation. In this case, a slightly less perfect fit was obtained giving an effective jelly roll thermal conductivity of 0.00515 W cm°K. This indicates a gain of only 7% in the thermal conductivity with very little change in the heat flow characteristics of the cell. This is clearly an inadequate improvement in the situation and cannot possibly form the basis of a practical solution to the BC cell thermal management problem.

6.4 Alternative Thermal Management

In a practical electric vehicle battery it would be feasible to cool the individual cells by circulating externally a suitable cooling fluid. It has already been determined from experimental test that ability of this external heat sinking technique to limit the internal jelly roll temperature rise is marginal. The radial cooling model gives a core temperature rise of 180°C under short circuit conditions. This peak temperature obviously occurs at a position furthest from the heat sink ie. in this case, at the mandrel. Since we cannot alter the thermal conductivity of the jelly roll there is only one practical way to reduce this peak temperature.

This is to reduce the effective jelly roll path length to the heat sink. The most straightforward way to do this is to cool the mandrel as well as the outer can. This case has therefore been analyzed to determine the expected temperature rise under conditions of high thermal power dissipation.

The steady state temperature distribution in a hollow cylinder is given by the equation

$$T(r) = \frac{-Go\ r^2}{4K} + A\ln r + B, \quad a \leq r \leq b \qquad *$$

A and B are constants determined by the surface temperatures T(a) and T(b) and the surface transfer coefficients. Go is the heat generation rate per unit volume (W/ml).

The peak temperature is at a radius and peak given by

$$r_{peak} = \sqrt{\frac{2AK}{Go}}$$

Values for T (r peak) for specific mandrel sizes and boundary conditions during short circuit discharge were calculated and are given in Table 8. The T values are calculated for a heat sink mandrel and can, using a fluid at 0°C. They therefore represent the expected temperature rise in the jelly roll. Note that a thermal power dissipation of 170 W was assumed for these calculations. For the reason giver earlier, the actual value will be lower depending upon the cell peak temperature.

---

* Carslaw, H.S., and Jaeger, J.C., Conduction of Heat in Solids, Oxford University Press, 1959

TABLE 8 - PEAK TEMPERATURE CALCULATED FOR VARIOUS CONDITIONS

Boundary Conditions	Mandrel Radius (cm)	T (r peak) (°C)
Forced Convection - fluid	0.3175 (Standard)	105
	0.45	94
Forced Convection - air	0.3175	118
	0.6	93

These results clearly indicate that temperature control of a BC cell is possible under short circuit conditions. The benefits from a modest increase in mandrel diameter are extremely encouraging although there is an added complexity to incorporate cooling passages in the mandrel. Even using air cooling it is possible to constrain the temperature rise within safe limits. In a practical system it would be necessary to analyze the trade-off of weight of cooling fluid vs the extra energy needed to circulate air coolant.

The individual cell design has to provide for removal of the high thermal power levels accompanying a short circuit in one cell and the foregoing has indicated that a suitable design is feasible. The cooling system however, has to handle the integrated power dissipation of the whole battery pack under peak load conditions. Data given in Section 6.1 show that this is 55 W per cell for a battery defined in Section 7.2 as comprising 180 BC MOLICELs. This is not a constant thermal power and therefore a system optimization would be necessary to size the cooling system and define the battery operational temperature range. This analysis would also have to include provision for passenger compartment heating. If the battery were to be undergoing cycle 1 of Figure 20 it is straightforward to estimate that a mean thermal power of 2.5 kW would have to be dissipated. If this were available at a temperature of 30 to 40°C then it could contribute significantly to passenger comfort in colder climates.

7. COMPARATIVE BATTERY PERFORMANCE IN ELECTRIC VEHICLE APPLICATIONS

7.1 EV Performance Estimation

From the point of view of this study, the critical parameters in regard to EV applications have been considered as performance and range. Aspects of cycle life and costs have not been considered.

In a vehicle propelled by an internal combustion engine (I.C.E.) the performance is limited only by the engine power. The range is limited by the fuel tank capacity. In an electric vehicle, the performance is limited by the battery capability. Generally the performance is acceptable only so long as the battery can meet the power requirements of the motor. The attainable battery power depends on the state of charge, size and temperature. Furthermore, the power and energy capabilities are not independent. See for example Figure 18. Thus the effective vehicle range depends upon the duty cycle. It is easy to see that the sizing of battery capacity, motor power and vehicle curb weight for a specific requirement becomes a complex multiparameter problem. In the performance tests herein, emphasis has been placed on the dynamic characteristics of MOLICELs. Too often, the designer is faced with only constant current discharge data for the battery. Since the real life situation imposes frequent up and down variations in battery drain rate it is necessary to know how this influences the battery performance and total delivered energy in order to make meaningful assessments of the proposed vehicle performance.

One way to relate the measured battery characteristics to the vehicle performance has been developed by F. Hornstra at Argonne National Laboratory[1]. The method requires a knowledge of the load profile to get the peak and the base specific power demands. The detailed structure of the load profile is unimportant. The required battery performance data are the Rogone plot (specific power vs. specific energy) and the plot of specific peak power vs. depth-of-discharge.

The specific power is used in conjunction with the Rogone plot to give the time to discharge, ie.

$$\text{time (hours)} = \frac{\text{Wh/Kg}}{\text{W/Kg}}$$

---

[1] F. HORNSTRA, First International Workshop on Battery Testing, Heidleberg, October, 1985, pp. 179.

Since the average velocity is known then the range can be calculated. This is the maximum range assuming only base power demand. What limits the range at the end of discharge is the inability of the battery to supply the peak power demand of the load profile. To determine the usable energy, the depth-of-discharge corresponding to the peak power demand is read off the plot of peak power vs. depth-of-discharge. The range is therefore reduced by a percentage equal to the percent depth-of-discharge just determined.

Figure 33 shows the load profile for the SAE J227(a) schedule D (velocity profile in dashed lines) required by the U.S. test vehicle IETV-1. It has a peak power of 47 W/Kg and a base power of 15 W/Kg. This vehicle carries 488 Kg of batteries. It will be seen from Figures 16 or 19 that the BC cell discharge time is 230 minutes at 15 W/Kg. The SAE J227(a) schedule D is 122 seconds long and the distance covered is 1.6 km. Therefore on one charge the vehicle would travel 180 km at constant power. According to the method defined here and the data read off Figure 12 this range is actually reduced to 85% in the practical cycle by the need to deliver peak power of 47 W/Kg. The range is therefore 154 km. Tests of this method at Argonne have shown that agreement with range data generated by full profile simulation is better than 6%. In all analyzes performed here the regenerative component of the cycle has been ignored. There is no information on the behavior of MOLICELs under such pulse charging conditions.

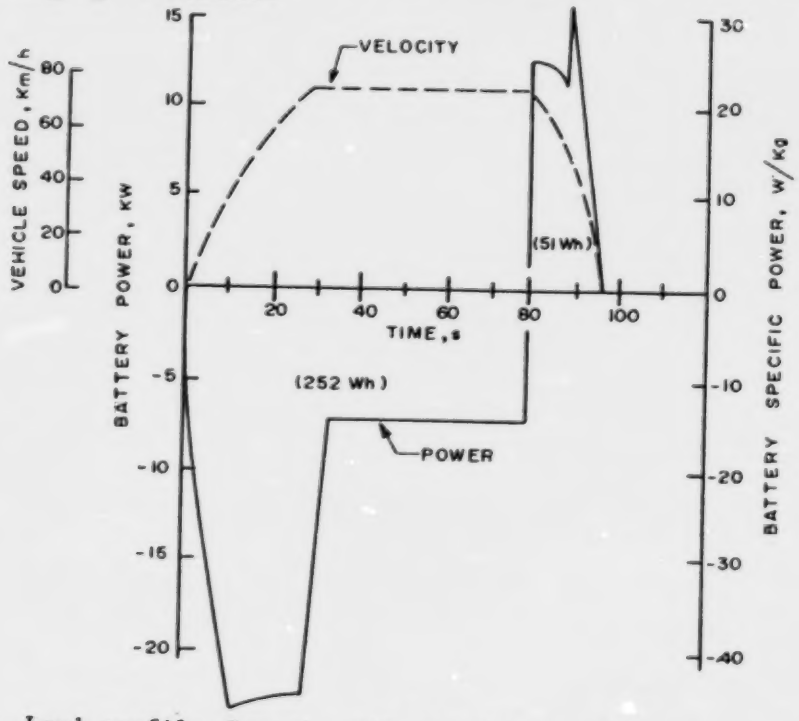

Figure 33: Load profile for the SAE J227(a) schedule D cycle for a U.S. test vehicle IETV-1. Regenerative component is shown but not included in calculations here. See text

7.2 Comparative Data

To assess the competitive viability of MOLICELs in EV applications, it is necessary to acquire reliable test results on other batteries. The data of Figure 34 are from Hornstra[2] plus BC cell results from the present study.

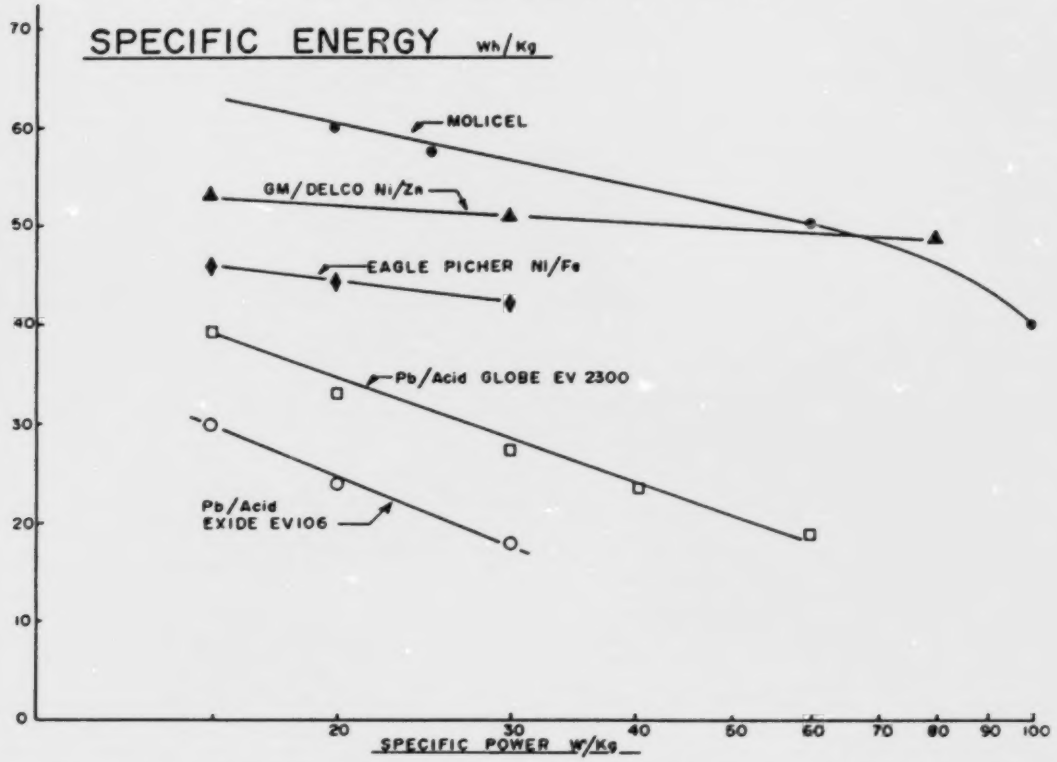

Figure 34: Specific energy vs. specific power for a number of possible E.V. batteries

Clearly over the power ranges required by the SAE J227(a) schedule D for the IETV-1 vehicle (15 to 47 W/Kg) the MOLICEL has superior specific energy. On Figure 35 some of the data are presented in the more familiar Rogone plot and Li/FeS data have been added from Barlow of Gould[3]. Here it is seen that the MOLICEL takes second place to the Li/FeS system which has an exceptionally high energy of 100 Wh/Kg at the required power range. It should be noted that at high powers the MOLICEL has superior performance.

---

[2] F. HORNSTRA, ibid, pp. 38.

[3] G. BARLOW, Proc. Intersoc. Energy Convers., Eng. Conf. 20, Vol. 2, 126 (1985).

Specific peak powers of a number of systems are compared on Figure 36 (data from references already given), and in a slightly different form in the Peukert plot of Figure 37. The negative limited Li/FeS system is relatively new and unproven. The more familiar positive limited system in fact has power performance inferior to MOLICELs. Over the power range covered by the requirements of the present example it is clear that the Pb/acid battery is an outstanding performer. Of course, reference to Figure 32 and 33 will soon reveal that in terms of energy the Pb/acid system is very inferior. The best Pb/acid system represented here would provide about half the range capability of a MOLICEL.

The EV designer has to take careful account of the battery characteristics otherwise the vehicle will not satisfy the performance requirements. However, in an understandable quest for maximizing the EV range to approach that of an I.C.E. vehicle, insufficient attention is given to the concept of optimizing the battery utilization. Reference to Figure 34 shows that BC size MOLICELs have energy densities of 40 Wh/Kg at >80W/Kg. This energy density is quite adequate to achieve acceptable range. The power capability can and should be used to advantage particularly as the duty cycle tests have shown that performance penalties are not incurred as a result of periodic but brief high peak power discharge levels. This suggests that optimized utilization of a BC cell battery can be

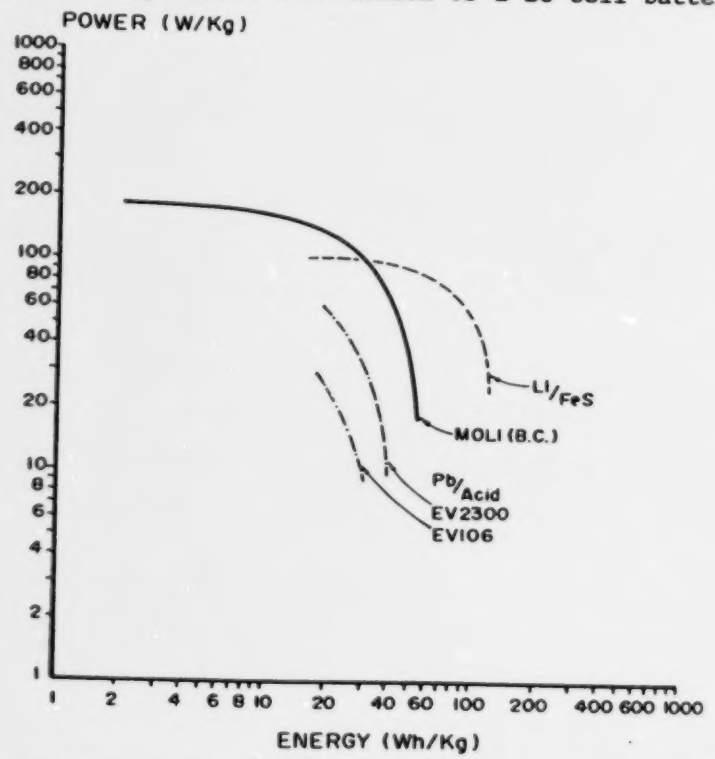

Figure 35: Specific power vs. specific energy for a number of possible E.V. batteries

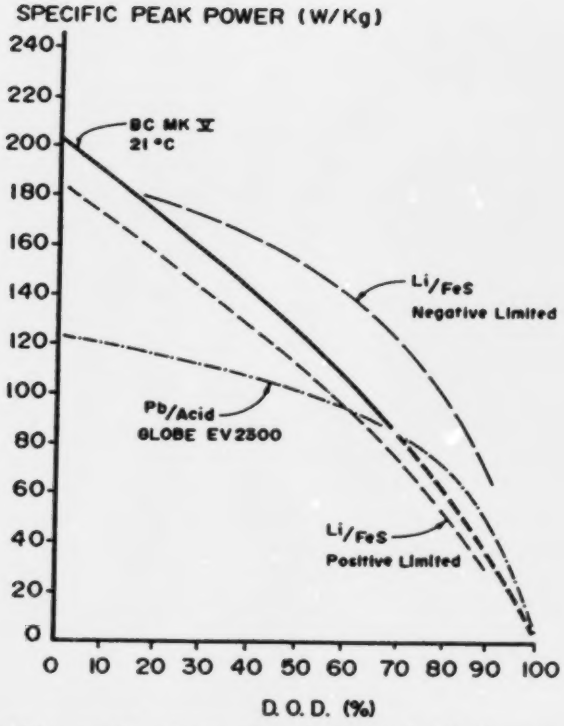

Figure 36: Specific peak power vs. depth-of-discharge for a number of possible E.V. batteries

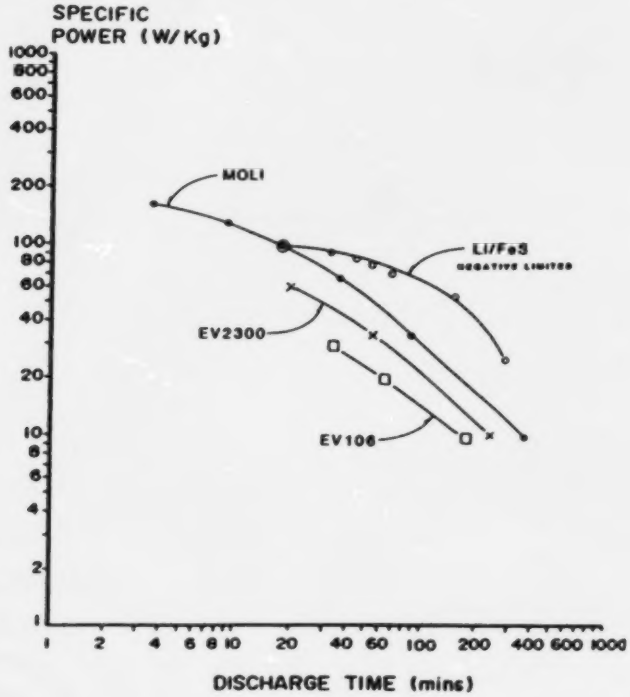

Figure 37: Peukert plot of several possible E.V. batteries

achieved using a relatively small battery fitted to a vehicle designed for limited range applications but having good acceleration, speed and hill climing capability.

To explore further the possibilities for such a vehicle the power requirements of a 1000 kg small, two passenger automobile have been calculated for execution of the SAE J227(a) schedules C and D. The results are given in Table 9, along with the relevant assumptions and conditions. Since the vehicle might reasonably be expected to perform additional maneuvers, consideration was given to passing and hill climbing. On a schedule D cycle, the power requirements become very large because of the higher speeds involved. therefore, data of Table 10 are confined only to the schedule C cycle. To keep total power requirements at reasonable levels the maximum grade selected was 6%. Passing required a top speed of 63 km/h to be completed in 19 seconds.

In order to define a duty cycle, the average of the peak powers for schedule C from Tables 9 and 10 were taken as the required peak power, ie. 17 kW. The base power was taken to be the road load plus losses at 48 km/h. This gives 6.7 kW. A battery of 180 BC MOLICELs could be fitted into the conceptual vehicle. The battery would weight 225 Kg. The individual cell peak power would be 94 W and the base power would be 37 W. This was the case tested in the duty cycle number 3 of 4.4 Table 5 and illustrated in Figure 20. The range achieved in actual test was 42 km (26 miles). It is noteworthy that the duty cycle tests show no range penalty associated with the much higher power demands of cycle 1 which would provide desirable performance gains in an actual vehicle. The actual range of 42 km is very modest. However, a small size battery was chosen (16 kWh) to be compatible with good drivability and very adequate road performance.

TABLE 9 - VEHICLE PEAK POWER REQUIREMENTS

STANDARD SAE J227(A) CYCLES

	Accel. (Secs)	Max. Speed (km/h)	Road Load (kW)	Accel. (kW)	Loss (kW)	Total (kW)
SCHEDULE C	18	48	1.6	9.2	5.1	15.9
SCHEDULE D	28	72	3.7	14.2	8.4	26.3

Road Load is Rolling + Drag.
Rolling Coeff = $0.008 + 1x10^{-5}V + 8x10^{-8}V^2$
Drag Coeff x Frontal Area = 0.4 m^2

Loss Calculation:
Power Controller 90%
Friction 90%
Motor 85%

TABLE 10 - VEHICLE POWER REQUIREMENTS FOR GRADE AND PASSING

	Accel. (Secs)	Max. Speed (km/h)	Road Load (kW)	Accel. (kW)	Loss (kW)	Total (kW)
6% Grade on Schedule C (Length 1/2 km)	0	48	1.6	8.4	4.7	14.7 (37.5 s)
Passing On Schedule C	10	63	4.5	8	5.9	18.4 (19 s)